minimize suffering. All studies involving wild mice were performed in compliance with the US Government Principles for the Utilization and Care of Vertebrate Animals used in Testing, Research, and Training; the Public Health Service Policy on Humane Care and Use of Laboratory Animals; The Animal Welfare Act and amendment laws; the Animal Care Policies of the USDA; The Guide for the Care and Use of Laboratory Animals (7th Edition; National Research Council); and the guidelines of the Committee on the Care and Use of Laboratory Animals under an NIAID-approved animal study protocol, and all studies and procedures were reviewed and approved by the Institutional Animal Care and Use Committee of the NIH (Permit Number: ASP LMM 1).

Mice and mouse genomic DNA

C57BL/6NCrslc, BALB/cCrslc, and B10A/SgSnslc mice were purchased from Japan SLC, Inc., Hamamatsu, Japan. Breeding pairs of A/WySnJ mice were purchased from The Jackson Laboratory, Bar Harbor, ME. The mA3-deficient strain on the B6 background has been described [27,40]. All laboratory mice were housed and bred in the Experimental Animal Facilities at Kinki University School of Medicine under specific pathogen-free conditions. The isolation of genomic DNA from spleens was carried out with DNeasy blood and tissue kit (Qiagen, Inc., Hilden, Germany) according to the manufacturer's instructions.

DNA and RNA were separately isolated from animals and cell lines developed from wild mice and wild mouse-derived breeding colonies or inbred strains (Table S1). Many wild-derived mice were obtained from M. Potter (National Cancer Institute, Bethesda, MD). CAST/Rp mice were obtained from R. Elliott (Roswell Park Cancer Institute, Buffalo, NY). Cells from some wild mouse species were obtained from J. Rodgers (Baylor College of Medicine, Houston, TX) and from J. Hartley, M. Lander or S. Chattopadhyay (National Institute of Allergy and Infectious Diseases, Bethesda, MD) [61,62]. *M. cervicolor popaeus* mice and tissue samples were obtained from R. Callahan (National Cancer Institute). Mice or DNA samples of inbred lines of *M. castaneus* (CAST/EiJ) and *M. molossinus* were obtained from The Jackson Laboratory. *M. musculus* DNA samples were obtained from S. Chattopadhyay and H. Morse (National Institute of Allergy and Infectious Diseases). DNA samples from wild-trapped European *M. domesticus* were provided by M. Nachman (University of Arizona, Tucson). DNA samples from 5 wild-derived strains (BLG2, NJL, MSM, HMI, PGN2) were obtained from the National Institute of Genetics, Mishima, Japan. A set of *Nannomys* DNAs was obtained from Y. Cole and P. D'Eustachio (Departments of Biochemistry and Medicine, New York University, NY); these mice were classed into 4 species on the basis of skeletal features by J. T. Marshall (Smithsonian Natural History Museum, Washington, DC). DNA was isolated from cultured tail biopsies, spleen, or liver by standard protocols, and RNA was isolated from the spleen or liver using TRI-Reagent (Molecular Research Center, Cincinnati, OH) or by a guanidine chloride extraction method [63].

Mouse *Apobec3* sequences and the prediction of mRNA secondary structures

DNA containing the mouse *Apobec3* exon 5 and associated intron sequences was amplified using either one of the following forward primers: 5′-GGACAATGGTGGCAGGCGATTC-3′, 5′-GCATCTTTGTGGATGGGG-3′, and the reverse primer 5-TCATTCCTCAATGCTCCTCC-3′. PCR products were cloned into pCR2.1-TOPO (Invitrogen, Carlsbad, CA) before sequencing. The *Apobec3* region was amplified from genomic DNA of B6, BALB/c, B10A, and A/WySnJ mice using the forward primer 5′-TTACAAATTTTAGATACCAGGATTCTAAGCTTCAGG-AG-3′ and the reverse primer 5′-GTCCTTTATGTGGGTTC-CAAGGACC-3′. PCR products were treated with ExoSAP-IT (USB, Cleveland, OH) and directly sequenced with the above reverse primer. To determine the BALB/c genomic sequence of the *Apobec3* intron 5, the BALB exon 5–6 and BALB intron 5-Δ3′ plasmids (Figure 5) were sequenced by using BigDye Terminator V3.1 Cycle Sequencing Kit (Applied Biosystems, Foster City, CA) and an ABI PRISM 3100 Genetic Analyzer (Applied Biosystems) using the following primers: T7 promoter forward, 5′- TAATAC-GACTCACTATAGGG-3′; and V5 reverse, 5′-CGTAGAATC-GAGACCGAGGAGAGGGTTAGGGATAGGC-3′.

The secondary structure of a portion of the mA3 mRNA exon 5 was predicted with *mfold* [64,65].

Cell culture and DNA transfection

BALB/3T3 and human 293T cells were cultured in Dulbecco's modified Eagle medium supplemented with 10% heat-inactivated fetal bovine serum (Invitrogen). These cells were seeded at 1.0×10^5/well in a well of 6-well plates one day prior to transfection. DNA transfection was performed by using Lipofectamine 2000 (Invitrogen) according to the manufacturer's protocols. Mouse spleen cells were harvested as described previously for protein and RNA extractions [27]. At least three independent transfection experiments were performed in this study and representative results are shown in the figures.

Plasmid constructions

The expression plasmids, pFLAG-CMV2-*mA3*^{b}Δ5 harboring the mA3 cDNA derived from the Δ5 transcript of the B6 allele, pFLAG-CMV2-*mA3*^{d} harboring the cDNA derived from the 5+ transcript of the BALB/c allele, pFLAG-CMV2-*mA3*^{d}Δ5 harboring the cDNA derived from the Δ5 transcript of the BALB/c allele, and control pFLAG-CMV2-GFP have been described [27]. The genomic DNA encoding the mA3 exon 5 was amplified from B6 genome with the following primers: 5′-ACCTTGCTACATCTCGGTCCCTTC-CAGC-3′ and 5′-CTGCCCTCCACCCAGAACCTCGTCTC-TGG-3′. The above pFLAG-CMV2-*mA3*^{b}Δ5 was used as a PCR template with primers 5′-GCGAATGGACCCGCTAAGTGAA-GAGG-3′ and 5′-CTCAGAATCTCCTGAAGCTTAGAATCC-TGG-3′ to amplify the linearized plasmid with a gap between exons 4 and 6. The two PCR products above were treated with T4 polynucleotide kinase (TAKARA Bio, Otsu, Japan) and fused by using the DNA Ligation Kit ver.2.1 (TAKARA Bio) to construct the plasmid pFALG-CMV2-*mA3*^{b}, which expresses the 5+ mA3 cDNA derived from the B6 allele.

B6 or BALB/c genomic fragments harboring exons 4–7 and the intervening introns were amplified by PCR using either the B6 or BALB/c genomic DNA as a template and the common primers 5′-CACCAATTTAAAAAGTGTTGGAAGAAG-3′ and 5′-GTGGGAGGTCCATGACGTCCACCAGGATCCC-3′. Each amplified DNA product was cloned into a pcDNA3.2/V5/GW/D-TOPO cloning vector (Invitrogen) and designated as B6 or BALB exon 4–7, respectively. The above B6 or BALB exon 4–7 was used as a template with the primers 5′-CACCACCTTGC-TACATCTCGGTCC-3′ and 5′-GCAGAGATGCTTGACTC-GTTGGTTG-3′ or 5′-CACCACCTTGCTACATCCCGGTC-C-3′ and 5′-GCAGAGATGCTTGACTCGTTGGTTG-3′, respectively, for the amplification of B6 or BALB/c exons 5 and 6 and the intervening intron 5. Each PCR product was cloned into the pcDNA3.2/V5/GW/D-TOPO vector and designated as B6 or BALB exon 5–6. The DNA fragments harboring sequentially deleted *Apobec3* intron 5 were prepared by PCR using either one of the above B6 or BALB exon 5–6 plasmids as a common template

with the primer pairs A–F listed in Table S2. Each amplified DNA product was cloned into the pcDNA3.2/V5/GW/D TOPO vector to generate the expression plasmid shown in Figure 5B.

Reciprocal chimeras between the above B5 and BALB exon 5–6 plasmids were generated by amplifying a linearized plasmid DNA lacking the 3′ intron 5 and exon 6 using primer pair G, and by amplifying the insert fragment using primer pair H.

Site-directed mutagenesis was performed by employing the QuikChange Site-Directed Mutagenesis Kit (Stratagene, La Jolla, CA) using the following templates and primers, listed separately in Table S2: BALB 100bp intron 5 (3′-100bp) plasmid was used as a common template for the preparation of BALB C14T, BALB C88G, and BALB C153GG163A with primer pairs I, J, K, respectively: B6 100bp intron 5 (3′-100bp) plasmid was used as a template to make B6 T14C or B6 G88C with primer pair L or M, respectively. The resultant B6 T14C plasmid was used as a template with the same primer pair M employed for the generation of B6 G88C to make B6 T14C G88C. B6 T14C G88C was then used as a template for the generation of B6 T14C G88C G153C A163G by using primer pair O. Similarly, the above-used primer pairs were also utilized for the generation of B6 exon 5–6 T14C, B6 exon 5–6 T14C G88C, and B6 exon 5–6 T14C G88C G153C A163G mutants by using B6 exon 5–6 as a template. The B6 exon 5–6 plasmid was also used as a template with primer pairs M, P, and Q for making B6 exon 5–6 G88C, B6 exon 5–6 G153C, and B6 exon 5–6 A163G, respectively.

To make BALB ΔTCCT, 4 consecutive nucleotides within the repeat sequence, TCCT, were deleted from the BALB exon 4–7 plasmid by mutagenesis using primer pair R, listed in Table S2. BALB ΔTCCT or BALB exon 4–7 plasmid was used as a template with primer pair S to make BALB C741T ΔTCCT or BALB C741T, respectively. To introduce the TCCT sequence by mutagenesis and make B6+TCCT, B6 exon 4–7 plasmid was used as a template with primer pair T. B6+TCCT or B6 exon 4–7 was used as a template with primer pair U to generate B6 T741C+TCCT or B6 T741C, respectively. Similarly, the above produced B6 exon 4–7+TCCT or BALB exon 4–7 ΔTCCT plasmid was used as a template and G88C or C88G substitution was introduced with primer set M or J, respectively.

All resultant plasmids were entirely sequenced by using BigDye Terminator V3.1 Cycle Sequencing Kit with an ABI PRISM 3100 Genetic Analyzer. In order to normalize the transfection efficiency, a plasmid expressing the luciferase gene, p*luc*, based on the expression vector pGL3 (Promega, Madison, WI), was utilized. All the primers used in this study were purchased from Operon Biotechnologies, Tokyo, Japan.

Quantitative real-time PCR assays for endogenous mA3 transcripts

For the quantification of mA3 transcripts in mouse spleens, total RNA was extracted from each spleen with RNeasy Mini Kit (Qiagen). The RNA was then subjected to reverse transcription with PrimeScript RT reagent Kit (TAKARA Bio). Real-time PCR reactions were carried out with SYBR Premix Ex Taq II (TAKARA Bio) on an Applied Biosystems 7900HT Fast Real-Time PCR System (Applied Biosystems) with two different sets of *Apobec3*-specific primers: set 1, 5′-GTGTTGGAAGAAGTTT-GTGG-3′ (primer a) and 5′-CCTGAAGCTTAGAATCCTGG-3′ (primer b); and set 2, 5′-TTACAAATTTTAGATACCAG-GATTCTAAGCTTCAGGAG-3′ (primer c) and 5′-TTGGTT-GTAAAACTGCGAGTAAAATTCCTCTTCAC-3′ (primer d). The data were normalized with expression levels of β-actin mRNA to obtain ΔCt values, and ΔΔCt values were calculated.

Detection and quantification of the *mA3* transcripts and their splicing products

For the detection of endogenous mA3 transcripts in mouse spleen cells, the RT products and primer sets used for the real-time PCR were also utilized for PCR using KOD Dash DNA polymerase (Toyobo, Osaka, Japan). The PCR products were separated by 1% agarose gel electrophoresis and detected by staining with ethidium bromide. For splicing assays, BALB/3T3 cells were transfected with 1 μg of each plasmid harboring a genomic DNA fragment and 0.5 μg of p*luc* to normalize the transfection efficiency. Total RNA was extracted from the transfected cells using the RNeasy Mini Kit at 24 hours post-transfection. The total RNA was treated with DNase I, reverse transcribed with SuperScript III First Strand Synthesis System (Invitrogen), and the resultant cDNA was subjected to PCR detection using KOD Dash DNA polymerase with the following primers: 5′-TAATACGACTCACTATAGGG-3′ (primer g) and 5′-CGTAGAATCGAGACCGAGGAGAGGGTTAGGGATAG-GC-3′ (primer h), designed to hybridize the T7 promoter and V5 tag regions of the vector, respectively. Primer i, 5′-GGTC-TCCCAGAGACGAGGTTCTG-3′, was used to detect only the exon 5-containing transcript. For real-time PCR quantification of the *mA3* transcripts containing exon 5, primer j (5′-GTGGAT-GAAGAGCTGGAAGGGACCG-3′) was used along with the above primer g. Transcripts containing exon 6 were similarly quantified by using primer k (5′-CAACCAACGAGTCAAG-CATCTCTGC-3′) and the above primer h.

For RT-PCR detection of mA3 mRNA in cells transfected with an mA3 expression plasmid, the same RT product as was used for real-time PCR analyses was utilized with the above-described primer set 1 (a–b). The RT products made by PrimeScript RT reagent Kit were supposed to be relatively short in length because a mixture of oligo-dT and random 6-mers were used as primers in the RT reaction. Thus, in order to detect the full-length and Δ5 transcripts, the following primers, 5′-GGGAATTCGATGG-GACCATTCTGTCTGGGATGCAGCCATCGC-3′ (primer e) and 5′-GGGTCGACTCAAGACATCGGGGGTCCAAGCTG-TAGGTTTCC-3′ (primer f), were used along with newly synthesized RT products generated by the SuperScript III First Strand Synthesis System (Invitrogen). To quantify the mA3 transcripts in 293T cells transfected with an mA3 expression plasmid, one-third of the transfected cells were used for total RNA isolation using the RNeasy Mini Kit at 24 hours after transfection. The purified RNA was treated with 5 units of DNase I (TAKARA Bio) for 1 hour at 37°C to digest the transfected DNA and then reverse transcribed with the PrimeScript RT reagent Kit. The real-time PCR was performed as described above.

For RT-PCR analyses of mA3 transcripts generated by the *in vitro* transcription/translation system, the reaction was stopped by the addition of lysis buffer included in RNeasy Mini Kit after 30 or 60 min of incubation, and the transcribed products were purified with the above kit. After the treatment of the purified RNA with DNase I, the RT-PCR reaction was carried out with the above primer set 1. After electrophoresis, gel images were recorded with a FluorChem™ IS-8900 transilluminator and band intensities were analyzed with AlphaEase FC Stand Alone software (Alpha Innotech, San Leandro, CA).

Apobec3 splicing patterns for wild-derived mice were identified by RT-PCR to amplify a segment of mA3 RNA spanning exon 5 from total RNA using forward primer 5′-GGACCATTCTG-TCTGGGATGCAGCCATCG-3′ and reverse primer 5′-GG-TTGTAAAACTGCGAGTAAAATTCC-3′.

Luciferase assays

Luciferase assays for normalization of transfection efficiencies were performed by utilizing the Luciferase Assay System (Promega). The enzymatic activities were measured by Wallac 1420 ARVO^{TM} MX-2 Multilabel Counter (Perkin Elmer).

Pre-absorption of the antibody

A spleen from an *Apobec3* knock-out mouse [40] was homogenized in 1ml ice-cold phosphate-buffered saline (PBS). Four ml of ice-cold acetone was added to the homogenate, mixed, and incubated on ice for 30 min. The lysate was centrifuged at 10,000×*g* at 4°C for 10 min. The pellet was washed with ice-cold acetone once and dried completely at room temperature to make spleen extract powder. Two µl of anti-APOBEC3 NT antibody specific for the N-terminal portion of mA3 (Millipore, Billerica, MA) was added to 0.5ml of KTBT buffer (50 mM Tris-HCl, pH 7.5, 150 mM NaCl, 10 mM KCl, 1% Triton X-100) containing 10% (w/v) unimmunized sheep serum as a carrier, into which 3mg of the spleen extract powder was dissolved. The mixture was incubated overnight at 4°C with gentle rotation. After centrifugation at 10,000×*g* at 4°C for 10 min, the supernatant was used as a pre-absorbed anti-mA3 antibody.

Immunoblotting

Western blotting analyses were conducted as described previously [27] with some modifications. Briefly, proteins were extracted with a lysis buffer (1% Nonidet P-40, 25 mM Tris-HCl, pH 7.5, 140 mM NaCl, 1 mM EDTA, 10 mM $Na_4P_2O_7$) containing protease inhibitors from Complete, Mini, EDTA-free Protease Inhibitor Cocktail Tablets (Roche Applied Science, Mannheim, Germany) and a phosphatase inhibitor, PhosSTOP (Roche Applied Science). Total protein concentrations were determined by Bradford assay (Nacalai Tesque, Kyoto, Japan) and the extracts were mixed with sodium dodecyl sulfate (SDS)-polyacrylamide gel electrophoresis (PAGE) sample buffer and heated at 95°C for 5 min. The proteins were separated by SDS-PAGE, transferred to Immobilon-P membrane (Millipore), and the blotted membranes were blocked with 5% (w/v) skim milk (Wako Pure Chemicals, Osaka, Japan) in Tris-buffered saline with 0.05% Tween 20 (TBST). The blocked membranes were incubated with the primary antibody at 4°C overnight. Membranes were then washed with TBST and incubated with horse radish peroxidase (HRP)-conjugated secondary antibody for 2 hours at room temperature, washed again with TBST, and the bound antibodies were detected using ECL plus reagent (GE Healthcare, Tokyo, Japan). The images were captured with a LAS-1000 Plus (Fujifilm, Tokyo, Japan) and the band intensities evaluated with Image Gauge ver. 3.12 (Fujifilm). A 1/5 dilution of the above-mentioned pre-absorbed mA3 antibody was made with IMMUNO SHOT (COSMO BIO, Tokyo, Japan) and was used as a primary antibody. Anti-FLAG M2 monoclonal antibody (mAb) (Sigma-Aldrich), anti-IκBα mAb (L35A5) (Cell Signaling Technology, Beverly, MA), anti-actin antibody (C-11) (Santa Cruz, CA), and the His-probe (H-15) (Santa Cruz) were diluted at 1:1000 with TBST. HRP-conjugated rabbit anti-mouse IgG (Zymed, South San Francisco, CA) and HRP-conjugated Goat anti-rabbit IgG antibodies (Invitrogen) were also diluted at 1:1000 and used as secondary antibodies to detect each appropriate primary antibody.

Assessment of mA3 protein stability

1.0×10^5 of 293T cells were transfected with 0.1 µg of an mA3 expression plasmid, 0.01 µg pFLAG-CMV2-GFP, and 0.1 µg of p*luc*. After 24h, the cells were treated with 10 µg/ml of cycloheximide or its solvent dimethyl sulfoxide (DMSO) as a control for 0, 2, or 4 hours. The cells were washed and resuspended in PBS. One-tenth of the cell suspension was subjected to luciferase assays to normalize transfection efficiencies, and the remaining cells were dissolved in the SDS-PAGE sample buffer. The normalized amount of cell lysates were separated by SDS-PAGE followed by immunoblotting as described above.

In vitro transcription and translation

The FLAG-mA3 cDNA was amplified with highly proofreading Pfu Turbo DNA Polymerase (Stratagene) from the plasmids pFLAG-CMV-*mA3^d* and pFLAG-CMV-*mA3^{d}Δ5* [27], with a forward primer harboring the T7 promoter sequence, 5′-GGATCCTAATACGACTCACTATAGGGAACAGCTGGGA-TGGGACCATTCTGTCTGGGATGC-3′ and a reverse primer harboring the His-Tag sequence, 5′-TCAATGGTGATGGT-GATGATGAGCAGCAGCAGACATCGGGGGTCCAAGCTG-TAGG-3′. The PCR products were subjected to reactions for *in vitro* transcription and translation using TNT T7 Quick for PCR DNA (Promega) according to the manufacturer's protocol. Half of the generated products were mixed with the SDS-PAGE sample buffer and analyzed by immunoblotting. The remaining products were used for RNA purification with RNeasy Mini Kit (Qiagen) followed by RT-PCR to detect mA3 transcripts.

Supporting Information

Figure S1 Nucleotide sequence of the genomic region encoding mA3 exon 5 and segments of flanking introns from several laboratory mouse strains and wild mouse species. Mouse *Apobec3* exon 5 and the flanking introns from 39 mice that represent different taxa or members of the same species trapped in different geographic locations, as well as those from the inbred laboratory strains BALB/c, B10.A, and A/WySn, were sequenced and aligned with the corresponding B6 sequence. The exon 5 and six key polymorphic regions, C/T741 and TCCT repeat in intron4, C/T14 and C/G88 in exon5, and C/G153 and A/G163 in intron 5, are indicated. Accession numbers for all newly obtained sequence data are also provided in this figure.
(PDF)

Figure S2 Possible stem-loop structures predicted from the mA3 intron 5 mRNA sequence. The mRNA secondary structures of exon 5 encoded by the B6 and BALB/c alleles were predicted by using the mfold [64,65]. Polymorphic nucleotides within this exon, U/C at position 14 and G/C at position 88, are indicated.
(PDF)

Table S1 Designations and sources of wild-derived mice, their cells, and DNA samples.
(PDF)

Table S2 Primers used to generate intron 5 deletion mutants and chimeras, for exon 5/intron 5 nucleotide substitutions, and for modification of TCCT repeat and T/C 741 SNP in intron 4.
(PDF)

Acknowledgments

We thank Drs. Sachiyo Tsuji-Kawahara, Eiji Kajiwara, and Shiki Takamura for their helpful discussions and comments and Mr. J. Brian Dowell for critically reading and correcting the manuscript. We thank Alicia Buckler-White for DNA sequencing. We are also grateful to the National Institute of Genetics, Mishima, Japan, for the provision of genomic DNA samples from wild mouse strains.

Author Contributions

Conceived and designed the experiments: MM. Performed the experiments: JL YH ET QL CAK. Analyzed the data: YI CAK MM. Contributed reagents/materials/analysis tools: CAK MM. Wrote the paper: YH CAK MM.

References

1. Bogerd HP, Wiegand HL, Doehle BP, Lueders KK, Cullen BR (2006) APOBEC3A and APOBEC3B are potent inhibitors of LTR-retrotransposon function in human cells. Nucleic Acids Res 34: 89–95.
2. Bogerd HP, Wiegand HL, Hulme AE, Garcia-Perez JL, O'Shea KS, et al. (2006) Cellular inhibitors of long interspersed element 1 and Alu retrotransposition. Proc Natl Acad Sci USA 103: 8780–8785.
3. Chen H, Lilley CE, Yu Q, Lee DV, Chou J, et al. (2006) APOBEC3A is a potent inhibitor of adeno-associated virus and retrotransposons. Curr Biol 16: 480–485.
4. Esnault C, Heidmann O, Delebecque F, Dewannieux M, Ribet D, et al. (2005) APOBEC3G cytidine deaminase inhibits retrotransposition of endogenous retroviruses. Nature 433: 430–433.
5. Esnault C, Millet J, Schwartz O, Heidmann T (2006) Dual inhibitory effects of APOBEC family proteins on retrotransposition of mammalian endogenous retroviruses. Nucleic Acids Res 34: 1522–1531.
6. Esnault C, Priet S, Ribet D, Heidmann O, Heidmann T (2008) Restriction by APOBEC3 proteins of endogenous retroviruses with an extracellular life cycle: *ex vivo* effects and *in vivo* "traces" on the murine IAPE and human HERV-K elements. Retrovirology 5: 75.
7. Harris RS, Bishop KN, Sheehy AM, Craig HM, Petersen-Mahrt SK, et al. (2003) DNA deamination mediates innate immunity to retroviral infection. Cell 113: 803–809.
8. Lochelt M, Romen F, Bastone P, Muckenfuss H, Kirchner N, et al. (2005) The antiretroviral activity of APOBEC3 is inhibited by the foamy virus accessory Bet protein. Proc Natl Acad Sci USA 102: 7982–7987.
9. Mangeat B, Turelli P, Caron G, Friedli M, Perrin L, et al. (2003) Broad antiretroviral defence by human APOBEC3G through lethal editing of nascent reverse transcripts. Nature 424: 99–103.
10. Mariani R, Chen D, Schrofelbauer B, Navarro F, Konig R, et al. (2003) Species-specific exclusion of APOBEC3G from HIV-1 virions by Vif. Cell 114: 21–31.
11. Navarro F, Bollman B, Chen H, Konig R, Yu Q, et al. (2005) Complementary function of the two catalytic domains of APOBEC3G. Virology 333: 374–386.
12. Russell RA, Wiegand HL, Moore MD, Schafer A, McClure MO, et al. (2005) Foamy virus Bet proteins function as novel inhibitors of the APOBEC3 family of innate antiretroviral defense factors. J Virol 79: 8724–8731.
13. Sasada A, Takaori-Kondo A, Shirakawa K, Kobayashi M, Abudu A, et al. (2005) APOBEC3G targets human T-cell leukemia virus type 1. Retrovirology 2: 32.
14. Schumacher AJ, Hache G, Macduff DA, Brown WL, Harris RS (2008) The DNA deaminase activity of human APOBEC3G is required for Ty1, MusD, and human immunodeficiency virus type 1 restriction. J Virol 82: 2652–2660.
15. Sheehy AM, Gaddis NC, Choi JD, Malim MH (2002) Isolation of a human gene that inhibits HIV-1 infection and is suppressed by the viral Vif protein. Nature 418: 646–650.
16. Turelli P, Mangeat B, Jost S, Vianin S, Trono D (2004) Inhibition of hepatitis B virus replication by APOBEC3G. Science 303: 1829.
17. Vartanian JP, Guetard D, Henry M, Wain-Hobson S (2008) Evidence for editing of human papillomavirus DNA by APOBEC3 in benign and precancerous lesions. Science 320: 230–233.
18. Conticello SG, Thomas CJ, Petersen-Mahrt SK, Neuberger MS (2005) Evolution of the AID/APOBEC family of polynucleotide (deoxy)cytidine deaminases. Mol Biol Evol 22: 367–377.
19. Jarmuz A, Chester A, Bayliss J, Gisbourne J, Dunham I, et al. (2002) An anthropoid-specific locus of orphan C to U RNA-editing enzymes on chromosome 22. Genomics 79: 285–296.
20. Malim MH (2009) APOBEC proteins and intrinsic resistance to HIV-1 infection. Philos Trans R Soc Lond B Biol Sci 364: 675–687.
21. Zhang H, Yang B, Pomerantz RJ, Zhang C, Arunachalam SC, et al. (2003) The cytidine deaminase CEM15 induces hypermutation in newly synthesized HIV-1 DNA. Nature 424: 94–98.
22. Lecossier D, Bouchonnet F, Clavel F, Hance AJ (2003) Hypermutation of HIV-1 DNA in the absence of the Vif protein. Science 300: 1112.
23. Iwatani Y, Chan DS, Wang F, Maynard KS, Sugiura W, et al. (2007) Deaminase-independent inhibition of HIV-1 reverse transcription by APOBEC3G. Nucleic Acids Res 35: 7096–7108.
24. Bishop KN, Verma M, Kim EY, Wolinsky SM, Malim MH (2008) APOBEC3G inhibits elongation of HIV-1 reverse transcripts. PLoS Pathog 4: e1000231.
25. Okeoma CM, Lovsin N, Peterlin BM, Ross SR (2007) APOBEC3 inhibits mouse mammary tumour virus replication in vivo. Nature 445: 927–930.
26. Santiago ML, Montano M, Benitez R, Messer RJ, Yonemoto W, et al. (2008) *Apobec3* encodes *Rfv3*, a gene influencing neutralizing antibody control of retrovirus infection. Science 321: 1343–1346.
27. Takeda E, Tsuji-Kawahara S, Sakamoto M, Langlois MA, Neuberger MS, et al. (2008) Mouse APOBEC3 restricts friend leukemia virus infection and pathogenesis in vivo. J Virol 82: 10998–11008.
28. Low A, Okeoma CM, Lovsin N, de las Heras M, Taylor TH, et al. (2009) Enhanced replication and pathogenesis of Moloney murine leukemia virus in mice defective in the murine APOBEC3 gene. Virology 385: 455–463.
29. Langlois MA, Kemmerich K, Rada C, Neuberger MS (2009) The AKV murine leukemia virus is restricted and hypermutated by mouse APOBEC3. J Virol 83: 11550–11559.
30. Jern P, Stoye JP, Coffin JM (2007) Role of APOBEC3 in genetic diversity among endogenous murine leukemia viruses. PLoS Genet 3: 2014–2022.
31. Chesebro B, Miyazawa M, Britt WJ (1990) Host genetic control of spontaneous and induced immunity to Friend murine retrovirus infection. Annu Rev Immunol 8: 477–499.
32. Miyazawa M, Tsuji-Kawahara S, Kanari Y (2008) Host genetic factors that control immune responses to retrovirus infections. Vaccine 26: 2981–2996.
33. Tsuji-Kawahara S, Chikaishi T, Takeda E, Kato M, Kinoshita S, et al. (2010) Persistence of viremia and production of neutralizing antibodies differentially regulated by polymorphic APOBEC3 and BAFF-R loci in Friend virus-infected mice. J Virol 84: 6082–6095.
34. Santiago ML, Benitez RL, Montano M, Hasenkrug KJ, Greene WC (2010) Innate retroviral restriction by Apobec3 promotes antibody affinity maturation in vivo. J Immunol 185: 1114–1123.
35. Miyazawa M, Nishio J, Wehrly K, Chesebro B (1992) Influence of MHC genes on spontaneous recovery from Friend retrovirus-induced leukemia. J Immunol 148: 644–647.
36. Hakata Y, Landau NR (2006) Reversed functional organization of mouse and human APOBEC3 cytidine deaminase domains. J Biol Chem 281: 36624–36631.
37. Sanville B, Dolan MA, Wollenberg K, Yan Y, Martin C, et al. (2010) Adaptive evolution of *Mus Apobec3* includes retroviral insertion and positive selection at two clusters of residues flanking the substrate groove. PLoS Pathog 6: e1000974.
38. Okeoma CM, Petersen J, Ross SR (2009) Expression of murine *APOBEC3* alleles in different mouse strains and their effect on mouse mammary tumor virus infection. J Virol 83: 3029–3038.
39. Santiago ML, Smith DS, Barrett BS, Montano M, Benitez RL, et al. (2011) Persistent Friend virus replication and disease in Apobec3-deficient mice expressing functional B-cell-activating factor receptor. J Virol 85: 189–199.
40. Mikl MC, Watt IN, Lu M, Reik W, Davies SL, et al. (2005) Mice deficient in APOBEC2 and APOBEC3. Mol Cell Biol 25: 7270–7277.
41. Hatakeyama S, Kitagawa M, Nakayama K, Shirane M, Matsumoto M, et al. (1999) Ubiquitin-dependent degradation of IκBα is mediated by a ubiquitin ligase Skp1/Cul1/F-box protein FWD1. Proc Natl Acad Sci USA 96: 3859–3863.
42. Teeter KC, Thibodeau LM, Gompert Z, Buerkle CA, Nachman MW, et al. (2010) The variable genomic architecture of isolation between hybridizing species of house mice. Evolution 64: 472–485.
43. Kozak CA, O'Neill RR (1987) Diverse wild mouse origins of xenotropic, mink cell focus-forming, and two types of ecotropic proviral genes. J Virol 61: 3082–3088.
44. Orth A, Adama T, Din W, Bonhomme F (1998) Natural hybridization between two subspecies of the house mouse, *Mus musculus domesticus* and *Mus musculus castaneus*, near Lake Casitas, California. Genome 41: 104–110.
45. Abudu A, Takaori-Kondo A, Izumi T, Shirakawa K, Kobayashi M, et al. (2006) Murine retrovirus escapes from murine APOBEC3 via two distinct novel mechanisms. Curr Biol 1615: 1565–1570.
46. Okeoma CM, Low A, Bailis W, Fan HY, Peterlin BM, et al. (2009) Induction of APOBEC3 in vivo causes increased restriction of retrovirus infection. J Virol 83: 3486–3495.
47. Mußil B, Sauermann U, Motzkus D, Stahl-Henning C, Sopper S (2011) Increased APOBEC3G and APOBEC3F expression is associated with low viral load and prolonged survival in simian immunodeficiency virus infected rhesus monkeys. Retrovirology 8: 77.
48. Biasin M, Piacentini L, Lo Caputo S, Kanari Y, Magri G, et al. (2007) Apolipoprotein B mRNA-editing enzyme, catalytic polypeptide-like 3G: a possible role in the resistance to HIV of HIV-exposed seronegative individuals. J Infect Dis 195: 960–964.
49. Boursot P, Din W, Anand R, Darviche D, Dod B, et al. (1996) Origin and radiation of the house mouse: Mitochondrial DNA phylogeny. J Evolution Biol 9: 391–415.

50. Din W, Anand R, Boursot P, Darviche D, Dod D, et al. (1996) Origin and radiation of the house mouse: Clues from nuclear genes. J Evolution Biol 9: 519–539.
51. Sawyer SL, Emerman M, Malik HS (2004) Ancient adaptive evolution of the primate antiviral DNA-editing enzyme APOBEC3G. PLoS Biol 2: E275.
52. Stocking C, Kozak C (2008) Murine endogenous retroviruses. Cell Mol Life Sci 65: 3383–3398.
53. Tomonaga K, Coffin J (1998) Structure and distribution of endogenous nonecotropic murine leukemia viruses in wild mice. J Virol 72: 8289–8300.
54. Ogawa T, Tsuji-Kawahara S, Yuasa T, Kinoshita S, Chikaishi T, et al. (2011) Natural killer cells recognize Friend retrovirus-infected erythroid progenitor cells through NKG2D-RAE-1 interactions in vivo. J Virol 85: 5423–5435.
55. Yamanaka S, Balestra ME, Ferrell LD, Fan J, Arnold KS, et al. (1995) Apolipoprotein B mRNA-editing protein induced hepatocellular carcinoma and dysplasia in transgenic animals. Proc Natl Acad Sci USA 92: 8483–8497.
56. Okazaki I, Hiai H, Kakazu N, Yamada S, Muramatsu M, et al. (2003) Constitutive expression of AID leads to tumorigenesis. J Exp Med 197: 1173–1181.
57. Kozak CA (2010) The mouse "xenotropic" gammaretroviruses and their XPR1 receptor. Retrovirology 7: 101.
58. Kidd JM, Newman TL, Tuzun E, Kaul R, Eichler EE (2007) Population stratification of a common APOBEC gene deletion polymorphism. PLoS Genet 3: e63.
59. Cascalho M (2004) Advantages and disadvantages of cytidine deamination. J Immunol 172: 6513–6518.
60. Pham P, Bransteitter R, Goodman MF (2005) Reward versus risk: DNA cytidine deaminases triggering immunity and disease. Biochemistry 44: 2703–2715.
61. Hartley JW, Rowe WP (1975) Clonal cell lines from a feral mouse embryo which lack host-range restrictions for murine leukemia viruses. Virology 65: 128–134.
62. Lander MR, Chattopadhyay SK (1984) A *Mus dunni* cell line that lacks sequences closely related to endogenous murine leukemia viruses and can be infected by ecotropic, amphotropic, xenotropic, and mink cell focus-forming viruses. J Virol 52: 695–698.
63. Chirgwin JM, Przybyla AE, MacDonald RJ, Rutter WJ (1979) Isolation of biologically active ribonucleic acid from sources enriched in ribonuclease. Biochemistry 18: 5294–5299.
64. Zuker M, Mathews DH, Turner DH (1999) Algorithms and thermodynamics for RNA secondary structure prediction: A practical guide. In: Barciszewski J, Clark BFC, eds. RNA Biochemistry and Biotechnology. Dordrecht: Kluwer Academic Publishers. pp 11–43.
65. Mathews DH, Sabina J, Zuker M, Turner DH (1999) Expanded sequence dependence of thermodynamic parameters improves prediction of RNA secondary structure. J Mol Biol 288: 911–940.
66. Veyrunes F, Dobigny G, Yang F, O'Brien PCM, Catalan J, et al. (2006) Phylogenomics of the genus *Mus* (Rodentia: Muridae): extensive genome repatterning is not restricted to the house mouse. Proc R Soc B 273: 2925–2934.
67. Lundrigan BL, Jansa SA, Tucker PK (2002) Phylogenetic relationships in the genus *Mus*, based on paternally, maternally, and biparentally inherited characters. Syst Biol 51: 410–431.
68. Guenet JL, Bonhomme F (2003) Wild mice: an ever-increasing contribution to a popular mammalian model. Trends Genet 19: 24–31.

ANTIMICROBIAL AGENTS AND CHEMOTHERAPY, July 2009, p. 2940–2948
0066-4804/09/$08.00+0 doi:10.1128/AAC.01727-08

Vol. 53, No. 7

The Novel CXCR4 Antagonist KRH-3955 Is an Orally Bioavailable and Extremely Potent Inhibitor of Human Immunodeficiency Virus Type 1 Infection: Comparative Studies with AMD3100▽

Tsutomu Murakami,[1]† Sei Kumakura,[2]† Toru Yamazaki,[2] Reiko Tanaka,[3] Makiko Hamatake,[1] Kazu Okuma,[3]‡ Wei Huang,[4] Jonathan Toma,[4] Jun Komano,[1] Mikiro Yanaka,[2]§ Yuetsu Tanaka,[3] and Naoki Yamamoto[1]*

AIDS Research Center, National Institute of Infectious Diseases, Tokyo 162-8640,[1] Biomedical Research Laboratories, Kureha Corporation, Tokyo 169-8503,[2] and Department of Immunology, Graduate School and Faculty of Medicine, University of the Ryukyus, Nakagami, Okinawa 903-0215,[3] Japan, and Monogram Biosciences, South San Francisco, California 94080[4]

Received 30 December 2008/Returned for modification 12 February 2009/Accepted 7 May 2009

The previously reported CXCR4 antagonist KRH-1636 was a potent and selective inhibitor of CXCR4-using (X4) human immunodeficiency virus type 1 (HIV-1) but could not be further developed as an anti-HIV-1 agent because of its poor oral bioavailability. Newly developed KRH-3955 is a KRH-1636 derivative that is bioavailable when administered orally with much more potent anti-HIV-1 activity than AMD3100 and KRH-1636. The compound very potently inhibits the replication of X4 HIV-1, including clinical isolates in activated peripheral blood mononuclear cells from different donors. It is also active against recombinant X4 HIV-1 containing resistance mutations in reverse transcriptase and protease and envelope with enfuvirtide resistance mutations. KRH-3955 inhibits both SDF-1α binding to CXCR4 and Ca^{2+} signaling through the receptor. KRH-3955 inhibits the binding of anti-CXCR4 monoclonal antibodies that recognize the first, second, or third extracellular loop of CXCR4. The compound shows an oral bioavailability of 25.6% in rats, and its oral administration blocks X4 HIV-1 replication in the human peripheral blood lymphocyte-severe combined immunodeficiency mouse system. Thus, KRH-3955 is a new promising agent for HIV-1 infection and AIDS.

The chemokine receptors CXCR4 and CCR5 serve as major coreceptors of human immunodeficiency virus type 1 (HIV-1), along with CD4 as a primary receptor for virus entry (2, 15, 18, 19). SDF-1α, which is a ligand for CXCR4, blocks the infection of CXCR4-utilizing X4 HIV-1 strains (7, 34). On the other hand, ligands for CCR5 such as RANTES inhibit CCR5-utilizing R5 HIV-1 (10). These findings made chemokines, chemokine derivatives, or small-molecule inhibitors of chemokine receptors attractive candidates as a new class of anti-HIV-1 agents. Many CCR5 antagonists have been developed as anti-HIV-1 drugs. These include TAK-779 (Takeda Pharmaceutical Company) (5), TAK-652 (6), TAK-220 (45), SCH-C (Schering-Plough) (43), SCH-D (vicriviroc) (42), GW873140 (aplaviroc; Ono Pharmaceutical/Glaxo Smith Kline) (28), and UK-427,857 (maraviroc; Pfizer Inc.) (17). Of these, maraviroc was approved by the U.S. FDA in 2007 for the treatment of R5 HIV-1 in treatment-experienced adult patients, combined with other antiretroviral treatment. Several classes of CXCR4 antagonists have also been reported. The bicyclam AMD3100 showed antivirus activity against many X4 and some R5X4 HIV strains in peripheral blood mononuclear cells (PBMCs) but not against R5 strains (16, 40). The pharmacokinetics and antiviral activity of this compound were also evaluated in humans (21, 22). T22, [Tyr-5,12, Lys-7]polyphemusin II, which is an 18-mer peptide derived from horseshoe crab blood cells, was reported to specifically inhibit X4 HIV-1 strains (30). Studies on the pharmacophore of T140 (a derivative of T22) led to the identification of cyclic pentapeptides (46).

In 2003, we reported that KRH-1636 is a potent and selective CXCR4 antagonist and inhibitor of X4 HIV-1 (23). Although the compound was absorbed efficiently from the rat duodenum, it has poor oral bioavailability. Continuous efforts to find more potent CXCR4 antagonists that are bioavailable when administered orally allowed us to develop KRH-3955 by a combination of chemical modification of the lead compound and biological assays. In this report, we describe the results of a preclinical evaluation of KRH-3955, including its in vitro anti-HIV-1 activity, its in vivo efficacy in the human peripheral blood lymphocyte (hu-PBL)-severe combined immunodeficiency (SCID) mouse model, and its pharmacokinetics in rats in comparison with those of AMD3100.

* Corresponding author. Mailing address: AIDS Research Center, National Institute of Infectious Diseases, 1-23-1 Toyama, Shinjuku-ku, Tokyo 162-8640, Japan. Phone: 81-3-5285-1111, ext. 2302. Fax: 81-3-5285-1165. E-mail: nyama@nih.go.jp.

† T.M. and S.K. contributed equally to this work.

‡ Present address: Department of Safety Research on Blood and Biological Products, National Institute of Infectious Diseases, Gakuen 4-7-1, Musashimurayama-shi, Tokyo 208-0011, Japan.

§ Present address: Kureha Special Laboratory Co., Ltd., Fukushima 974-8232, Japan.

▽ Published ahead of print on 18 May 2009.

MATERIALS AND METHODS

Compounds. The synthesis and purification of KRH-3955, *N*,*N*-dipropyl-*N*′-[4-({[(1*H*-imidazol-2-yl)methyl][(1-methyl-1*H*-imidazol-2-yl)methyl]amino}methyl)benzyl]-*N*′-methylbutane-1,4-diamine tri-(2*R*,3*R*)-tartrate, were carried out by Kureha Corporation. The chemical structure of KRH-3955 is shown in Fig. 1. The CXCR4 antagonist AMD3100 and zidovudine (AZT) were obtained from Sigma. Saquinavir was obtained

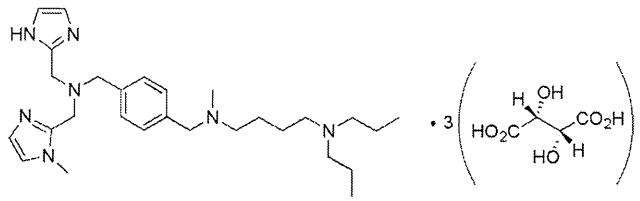

FIG. 1. Chemical structure of KRH-3955.

from the NIH AIDS Research and Reference Reagent Program, NIAID, Bethesda, MD. AMD070 and SCH-D were synthesized at Kureha Corporation.

Cells. Molt-4 no. 8 cells (24) were maintained in RPMI 1640 medium (Invitrogen, Carlsbad, CA) supplemented with 10% fetal bovine serum (Sigma, St. Louis, MO) and antibiotics (50 ng/ml penicillin, 50 ng/ml streptomycin, and 100 ng/ml neomycin; Invitrogen), which is referred to as RPMI medium. Chemokine receptor-expressing human embryonic kidney 293 (HEK293) cells (ATCC CRL-1573) and Chinese hamster ovary (CHO) cells (ATCC CCL-61) were maintained in minimal essential medium or F-12 (Invitrogen) supplemented with 10% fetal bovine serum and antibiotics (50 ng/ml penicillin, 50 ng/ml streptomycin, and 100 ng/ml neomycin). PBMCs from HIV-1-seronegative healthy donors were isolated by Ficoll-Hypaque density gradient (Lymphosepal; IBL, Gunma, Japan) centrifugation (31) and grown in RPMI medium supplemented with recombinant human interleukin-2 (rhIL-2; Roche, Mannheim, Germany) at 50 U/ml.

Viruses. Viral stocks of HIV-1_{NL4-3}, HIV-1_{JR-CSF}, and HIV-$1_{89.6}$ were each produced in the 293T cell line by transfection with HIV-1 molecular clone plasmids pNL4-3 (1), pYK-JRCSF (25), and p89.6 (11), respectively, by the calcium phosphate method. The 50% tissue culture infective dose was determined by an end-point assay with PBMC cultures activated with immobilized anti-CD3 monoclonal antibody (MAb) (33, 51). Subtype B HIV-1 primary isolates 92HT593, 92HT599 (N. Hasley), and 91US005 (B. Hahn) and AZT-resistant HIV-1 (A018) (D. D. Richman) (26) were obtained from the AIDS Research and Reference Reagent Program, Division of AIDS, NIAID, NIH. These clinical isolates were propagated in the activated PBMCs prepared as described above.

Anti-HIV-1 assays. Human PBMCs activated with immobilized anti-CD3 MAb (OKT-3; ATCC, Manassas, VA) in RPMI medium for 3 days were infected with various HIV-1 strains, including primary clinical isolates, at a multiplicity of infection of 0.001. After 3 h of adsorption, the cells were washed and cultured in RPMI medium supplemented with rhIL-2 (50 U/ml) in the presence or absence of the test compounds. Amounts of HIV-1 capsid (p24) antigen produced in the culture supernatants were measured by an enzyme-linked immunosorbent assay kit (ZeptoMetrix Corp., Buffalo, NY) 7 to 10 days after infection. The cytotoxicities of the compounds were tested on the basis of the viability and proliferation of the activated PBMCs, as determined with Cell Proliferation Kit II (XTT) from Roche (36).

Susceptibility of multidrug-resistant HIV-1 to CXCR4 antagonists was also measured by using recombinant viruses in a single replication cycle assay (9, 49). HIV-1 resistance test vectors (RTVs) contain the entire protease (PR) coding region and the reverse transcriptase (RT) coding region, from amino acid 1 to amino acid 305, amplified from patient plasma and a luciferase expression cassette inserted in the *env* region. The RTVs in this study contain patient-derived PR and RT sequences that possess mutations associated with resistance to PR, RT, or both PR and RT. Env-pseudotyped viruses were produced by cotransfecting 293 cells with RTV plasmids and expression vectors encoding the Env protein of well-characterized X4-tropic laboratory strain HXB2, NL4-3, or NL4-3 containing the Q40H enfuvirtide (T20) resistance mutation introduced by site-direct mutagenesis. The virus stocks were harvested 2 days after transfection and used to infect U87 $CD4^+$ cells (kind gifted from N. Landau, NYU School of Medicine) expressing CXCR4 in 96-well plates, with serial dilutions of CXCR4 antagonists. Target cells were lysed, and luciferase activity was measured to assess virus replication in the presence and absence of inhibitors. Drug concentrations required to inhibit virus replication by 50% (IC_{50}) were calculated.

Immunofluorescence. Molt-4 cells or CXCR4-expressing HEK293 cells were treated with various concentrations of KRH-3955 or AMD3100 in RPMI medium or phosphate-buffered saline containing 1% bovine serum albumin and 0.05% NaN_3 (fluorescence-activated cell sorting [FACS] buffer). In washing experiments, cells were washed with RPMI medium or FACS buffer. The cells were Fc blocked with 2 mg/ml normal human immunoglobulin G (IgG) in FACS buffer and then stained directly with mouse MAbs 12G5-phycoerythrin (PE) and 44717-PE (R&D Systems, Inc., Minneapolis, MN) or rat MAb A145-fluorescein isothiocyanate (FITC) and indirectly with MAb A80. The A145 and A80 MAbs were produced in ascitic fluid of BALB/c nude mice, and IgG fractions were obtained from ascitic fluid by gel filtration chromatography with Superdex G200 (Amersham Pharmacia). Goat anti-rat IgG (heavy and light chains) labeled with FITC was purchased from American Corlex (47). After washing, the cells were analyzed on a FACScalibur (BD Biosciences, San Jose, CA) flow cytometer with CellQuest software (BD Biosciences).

DNA construction and transfection. Chemokine receptor-expressing CHO cells were generated as reported previously (23). Human CXCR4 cDNA was cloned into the pcDNA3.1 vector. Mutations were introduced by using the QuikChange II site-directed mutagenesis kit (Stratagene, La Jolla, CA). All constructs were verified by DNA sequencing and transfected into 293 cells by using the Lipofectamine reagent (Invitrogen) (48). Stable transfectants were selected in the presence of 400 μg/ml G418 (Invitrogen). The COOH-terminal intracellular domain of CXCR4 (residues 308 to 352) was deleted in all mutants and the wild type. This deletion has no influence on HIV-1 infection or on SDF-1α binding and signaling but abolishes ligand-induced endocytosis (3).

Ligand-binding assays. Chemokine receptor-expressing CHO cells (5×10^6/0.2 ml per well) were cultured in a 24-well microtiter plate. After 24 h of incubation at 37°C, the culture medium was replaced with binding buffer (RPMI medium supplemented with 0.1% bovine serum albumin). Binding reactions were performed on ice in the presence of ^{125}I-labeled chemokines (final concentration of 100 pmol/liter; PeproTech Inc., Rocky Hill, NJ) and various concentrations of test compounds. After washing away of unbound ligand, cell-associated radioactivity was counted with a scintillation counter as described previously (23).

CXCR4-mediated Ca^{2+} signaling. Fura2-acetoxymethyl ester (Dojindo Laboratories, Kumamoto, Japan)-loaded CXCR4-expressing CHO cells were incubated in the absence or presence of various concentrations of KRH-3955 or AMD3100. Changes in intracellular Ca^{2+} levels in response to SDF-1α (1 μg/ml) were determined by using a fluorescence spectrophotometer as described previously (30).

Detection of KRH-3955 in blood after oral administration. The plasma concentration-time profile of R-176211 (distilled water was used as a vehicle), the free form of KRH-3955, was examined after a single oral administration of KRH-3955 at a dose of 10 mg/kg or intravenous administration at a dose of 10 mg/kg to male Sprague-Dawley rats (CLEA, Kanagawa, Japan). R-176211 in plasma was measured by liquid chromatography-tandem mass spectrometry. Pharmacokinetic parameters were calculated by using WinNonlin Professional (ver. 3.1; Pharsight Co.).

Infection of hu-PBL–SCID mice. Two groups of C.B-17 SCID mice (CLEA, Kanagawa, Japan) were administered a single dose of either KRH-3955 or tartrate (2% glucose solution was used as the vehicle) as a control orally (p.o.) and fed for 2 weeks. These mice were then engrafted with human PBMCs (1×10^7 cells/animal intraperitoneally [i.p.]) and after 1 day were infected i.p. with 1,000 infective units of X4 HIV-1_{NL4-3}. IL-4 (2 μg per animal) was administrated i.p. on days 0 and 1 after PBMC engraftment to enhance X4 HIV-1 infection. After 7 days, human lymphocytes were collected from the peritoneal cavities and spleens of the infected mice and cultured in vitro for 4 days in RPMI medium supplemented with 20 U/ml rhIL-2. HIV-1 infection was monitored by measuring p24 levels in the culture supernatant. We used a selected donor whose PBMCs could be engrafted at an efficiency of >80% in C.B-17 SCID mice. Usually, 5×10^5 to 10×10^5 human $CD4^+$ T cells can be recovered from each hu-PBL–SCID mouse. Mice with no or low recovery of human $CD4^+$ T cells at the time of analysis were omitted. For ex vivo cultures, we used a quarter of the cells recovered from a mouse. The protocols for the care and use of the hu-PBL–SCID mice were approved by the Committee on Animal Research of the University of the Ryukyus before initiation of the present study.

RESULTS

Anti-HIV-1 activities of KRH-3955 in activated PBMCs. The inhibitory activity of KRH-3955 against X4 HIV-1 (NL4-3), R5X4 HIV-1 (89.6), and R5 HIV-1 (JR-CSF) was examined in activated human PBMCs from two different donors. KRH-3955 inhibited the replication of both X4 and R5X4 HIV-1 in activated PBMCs with 50% effective concentrations (EC_{50}) of 0.3 to 1.0 nM but did not affect R5 HIV-1 replication, even at concentration of up to 200 nM (Table 1). In contrast, the CCR5 antagonist SCH-D (vicriviroc) inhibited R5 HIV-1 rep-

TABLE 1. Anti-HIV-1 activity of KRH-3955 in activated PBMCs[a]

Virus	Donor	EC_{50} (nM)[b]					
		KRH-3955	AMD3100	AMD070	SCH-D	AZT	SQV
NL4-3	A	1.1	41	35	>1,000	11	9.0
X4	B	0.33	15	15	>1,000	8.0	29
89.6	A	0.38	44	55	>1,000	7.4	9.9
R5X4	B	ND[c]	ND	ND	ND	ND	ND
JR-CSF	A	>200	>200	>200	0.37	0.96	2.6
R5	B	>200	>200	>200	1.2	6.2	8.0
A018H (X4) (pre-AZT)	C	1.4	38	ND	ND	1.9	ND
A018G (X4) (post-AZT)	C	1.3	32	ND	ND	87,000	ND

[a] PBMCs from two different donors were used in each assay. Anti-HIV-1 activity was determined by measuring the p24 antigen level in culture supernatants.
[b] Assays were carried out in triplicate wells. The average of two to four experiments is shown.
[c] ND, not determined.

lication but inhibited neither X4 nor R5X4 HIV-1 replication (Table 1). The anti-HIV activity of KRH-3955 against the 89.6 virus from donor B was not determined because the virus did not replicate enough for calculation of the anti-HIV activity of KRH-3955 and other drugs. Notably, the anti-HIV-1 activity of KRH-3955 was much higher than that of AMD3100, a well-known X4 HIV-1 inhibitor, or AMD070, the other X4 inhibitor that is bioavailable when administered orally. KRH-3955 also inhibited the replication of clinical isolates of X4 HIV-1 (92HT599) and R5X4 HIV-1 (92HT593) with EC_{50} ranging from 4.0 to 4.2 nM (data not shown). Although both KRH-3955 and AMD3100 were effective against at least some R5X4 HIV-1 strains in activated PBMCs, neither KRH-3955 nor AMD3100 inhibited the infection of CD4/CCR5 cells by R5 or R5X4 HIV-1, even at a concentration of 1,660 nM (data not shown). Importantly, the 50% cytotoxic concentration of KRH-3955 in activated PBMCs (donor A) was 57 μM, giving a high therapeutic index (51,818) in the case of NL4-3 infection, which was higher than that of AZT (8,000 in the case of donor A). These results indicate that the compound is a selective inhibitor of HIV-1 that can utilize CXCR4 as a coreceptor. Since a CXCR4 antagonist should be used in combination with a CCR5 antagonist in a clinical setting, we next examined whether the combined use of both antagonists efficiently blocks mixed infection with X4 and R5 HIV-1. Combination of KRH-3955 and SCH-D at 4 plus 4 nM and 20 plus 20 nM blocked the replication of 50:50 mixtures of NL4-3 and JR-CSF by 91 and 96%, respectively (data not shown). Thus, KRH-3955 is a highly potent and selective inhibitor of X4 HIV-1.

Anti-HIV-1 activities of KRH-3955 in activated PBMCs from different donors. It has been observed that the anti-HIV-1 activity of compounds in PBMCs varies from donor to donor. Therefore, the anti-HIV-1 activity of KRH-3955 against X4 HIV-1 was examined in activated PBMCs from eight different donors. The levels of p24 antigen in NL4-3-infected cultures ranged from 17 to 120 ng/ml (Table 2). KRH-3955 inhibited the replication of NL4-3 with EC_{50} ranging from 0.23 to 1.3 nM and with EC_{90} ranging from 2.7 to 3.5 nM (Table 2), demonstrating that the anti-HIV-1 activity of KRH-3955 was independent of the PBMC donor.

Anti-HIV-1 activities of KRH-3955 against drug-resistant HIV-1 strains. To further assess the efficacy of KRH-3955, we used a single-cycle assay to evaluate the activity of KRH-3955 against a panel of recombinant viruses that express an X4-tropic envelope protein (HXB2) but contain PR and RT sequences containing a wide variety of mutations associated with resistance to PR inhibitors (PIs), nucleoside RT inhibitors (NRTIs), and non-NRTIs (NNRTIs). This assessment was also performed with recombinant viruses that express an X4-tropic envelope protein (NL4-3) that contains the Q40H mutation and displays resistance to T20 (an entry inhibitor). The results of these experiments demonstrate that both KRH-3955 and AMD3100 inhibited the infection of CD4/CXCR4 cells by these recombinant drug-resistant viruses, including viruses resistant to PIs, NRTIs, or NNRTIs; multidrug-resistant viruses; and T20-resistant viruses (Table 3). We also observed that KRH-3955 inhibited the replication of A018G, a highly AZT-resistant strain, in activated PBMCs with an EC_{50} of 1.3 nM (Table 1).

KRH-3955 selectively inhibits ligand binding to CXCR4. To investigate whether KRH-3955 specifically blocks ligand binding to CXCR4, the inhibitory effect of the compound on chemokine binding to CHO cells expressing CXCR4, CXCR1, CCR2b, CCR3, CCR4, or CCR5 was determined. KRH-3955 efficiently inhibited SDF-1α binding to CXCR4 in a dose-dependent manner (Fig. 2 and 3b), and the IC_{50} for SDF-1α binding was 0.61 nM, which is similar to its EC_{50} against HIV-1. Similar results were obtained when we used a Molt-4 T cell line as the CXCR4-expressing target cell (Fig. 3a). Interestingly, the inhibitory activity of AMD3100 against SDF-1α binding was much weaker than its anti-HIV-1 activity (Fig. 3), suggesting that the binding sites of these two compounds are different. In contrast, the compound did not affect the binding

TABLE 2. Anti-HIV-1 activity of KRH-3955 against NL4-3 infection of PBMCs from eight different donors

Donor	p24 level (ng/ml)	EC_{50} (nM)	EC_{90} (nM)
1	31	1.30	3.2
2	25	1.20	3.2
3	17	1.20	3.3
4	40	0.70	2.9
5	120	0.77	2.9
6	58	1.50	3.5
7	49	0.23	2.7
8	53	1.00	3.0
Mean ± SD	49 ± 32	0.99 ± 0.40	3.1 ± 0.30

TABLE 3. KRH-3955 susceptibilities of drug-resistant viruses[a]

Virus[b]	IC_{50} (nM)[c]	
	KRH-3955	AMD3100
NL4-3	0.50	4.6
HXB2	0.60	6.2
NRTI-Res (HXB2-env)	0.60	9.0
NNRTI-Res (HXB2-env)	0.80	7.0
PI-Res (HXB2-env)	0.70	9.2
MDR (HXB2-env)	0.70	5.3
T20-Res (NL4-3-env)	0.40	2.3

[a] Susceptibility of drug-resistant HIV-1 was measured by using a single-cycle recombinant virus assay (see Materials and Methods).
[b] The pseudoviruses containing X4-tropic envelope (HXB2 or NL4-3) and patient-derived PR and RT sequences containing mutations associated with resistance to PR (PI-Res), RT (NRTI-Res or NNRTI-Res), or both (MDR) (the mutations are not shown). T20-Res contains a site-directed mutation (Q40H) in the NL4-3 envelope.
[c] IC50, 50% inhibitory concentration of CXCR4 antagonists.

of ^{125}I-labeled SDF-1α, ^{125}I-labeled RANTES, ^{125}I-labeled MCP-1, ^{125}I-labeled TARC, ^{125}I-labeled RANTES, or ^{125}I-labeled IL-8 to CXCR4, CCR1, CCR2b, CCR4, CCR5, or CXCR1, respectively (Fig. 2). Thus, KRH-3955 selectively blocks the binding of SDF-1α to CXCR4.

KRH-3955 exhibits inhibition of Ca^{2+} signaling through CXCR4. We next examined whether KRH-3955 acts as an agonist or antagonist of CXCR4 by using CXCR4-expressing CHO cells. The addition of KRH-3955 inhibited the SDF-1α-induced increase in the intracellular Ca^{2+} concentration in a dose-dependent manner, whereas 100 nM AMD3100 did not affect Ca^{2+} mobilization (Fig. 4). KRH-3955 itself did not affect Ca^{2+} mobilization at up to 1 μM (data not shown). We performed the Ca^{2+} mobilization assay with human PBMCs but could not detect an SDF-1α-induced Ca^{2+} signal mainly due to low expression of CXCR4 (data not shown). Thus, KRH-3955 inhibits Ca^{2+} signaling through CXCR4.

Effect of KRH-3955 on anti-CXCR4 antibody binding to CXCR4-expressing cells. To localize the binding site(s) of KRH-3955, the effects of KRH-3955 and AMD3100 on the binding of four types of anti-CXCR4 MAbs were first examined. We used MAbs A145, 12G5, 44717, and A80, which are specific for the N terminus, extracellular loop 1 (ECL1) and ECL2, ECL2, and ECL3, respectively. Neither KRH-3955 nor AMD3100 inhibited A145 binding to CXCR4-expressing Molt-4 cells (Fig. 5). Both compounds inhibited the binding of MAbs 12G5, 44717, and A80 to Molt-4 cells in a dose-depen-

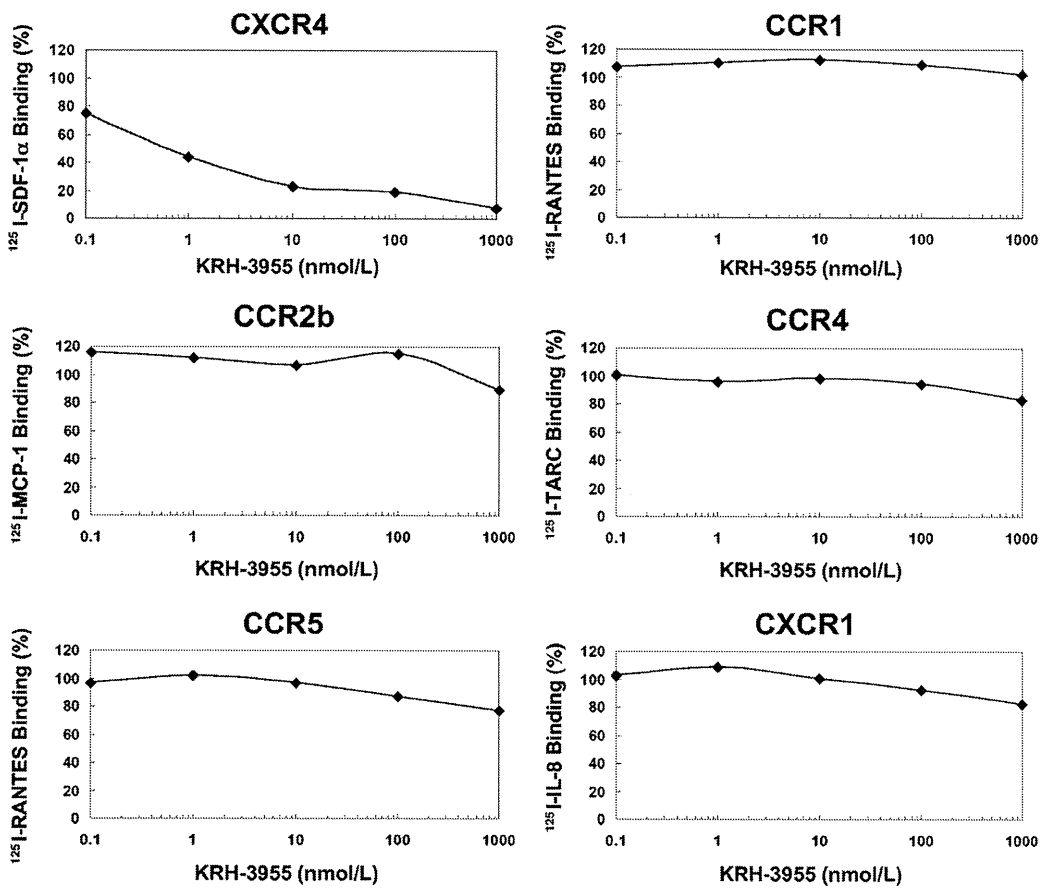

FIG. 2. Inhibitory effects of KRH-3955 on chemokine binding to CXCR4-, CCR1-, CCR2b-, CCR4-, CCR5-, or CXCR1-expressing CHO cells. Chemokine receptor-expressing CHO cells were incubated with various concentrations of KRH-3955 in binding buffer containing ^{125}I-labeled chemokine. Binding reactions were performed on ice and were terminated by washing out the unbound ligand. Cell-associated radioactivity was measured with a scintillation counter. Percent binding was calculated as 100 × [(binding with inhibitor − nonspecific binding)/(binding without inhibitor − nonspecific binding)]. The data represent the means in duplicate wells in a single experiment.

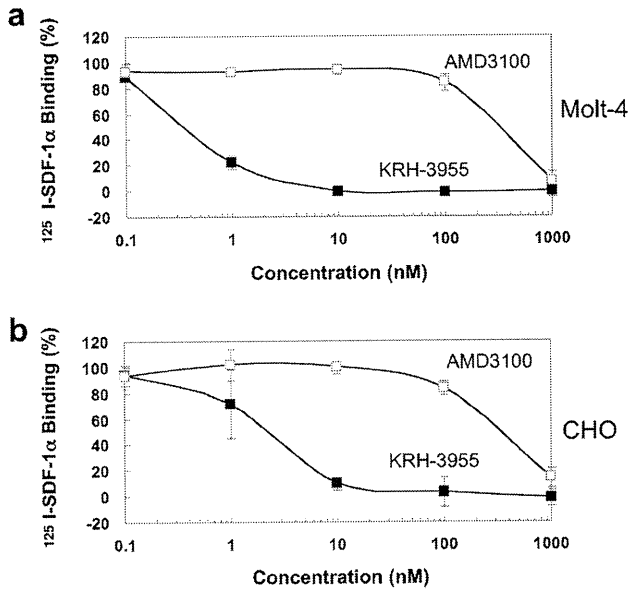

FIG. 3. Concentration-dependent inhibition by KRH-3955 of SDF-1α binding to (a) Molt-4 and (b) CXCR4-expressing CHO cells. CXCR4-expressing CHO cells were incubated with various concentrations of KRH-3955 (■) or AMD3100 (□) in binding buffer containing ^{125}I-labeled SDF-1α. Binding reactions were performed, and percent binding was calculated as described in the legend to Fig. 2. The data represent the means ± standard deviations of three independent experiments.

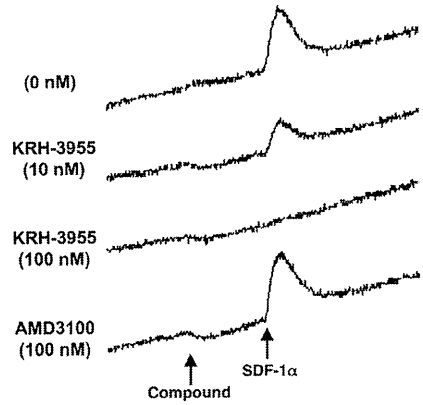

FIG. 4. Inhibitory effects of KRH-3955 on SDF-1α-induced Ca^{2+} mobilization in CXCR4-expressing CHO cells. Fura-2-acetoxymethyl ester-loaded CXCR4-expressing CHO cells were incubated in the presence or absence of various concentrations of KRH-3955 or AMD3100. Changes in intracellular Ca^{2+} levels in response to SDF-1α (1 μg/ml) were determined with a fluorescence spectrophotometer. The data show representative data for two independent experiments.

dent manner. The inhibitory activity of KRH-3955 is similar to its anti-HIV-1 activity, whereas the inhibitory activity of AMD3100 is much weaker than its anti-HIV-1 activity. Similar data were obtained when activated human PBMCs were used as target cells (data not shown). KRH-3955 itself did not induce internalization of CXCR4 at concentrations of up to 1 μM (data not shown), as KRH-1636 did (23). These results suggest that the binding sites of KRH-3955 are located in a region composed of all three ECLs of CXCR4.

Long-lasting inhibitory effects of KRH-3955 on the binding of MAb 12G5. The inhibitory effect of KRH-3955 on the binding of MAb 12G5 was examined with or without washing of the compound from the cells. Molt-4 cells were treated with 10 nM KRH-3955 or 1,000 nM AMD3100 for 15 min. With or without washing, the cells were stained with MAb 12G5-PE and the amount of bound antibody was analyzed by flow cytometry. KRH-3955 strongly inhibited MAb 12G5 binding to Molt-4 cells irrespectively of washing (Fig. 6a). In contrast, AMD3100 efficiently inhibited MAb 12G5 binding without washing away of the compound but lost its inhibitory activity after washing away of the compound (Fig. 6a). The long-lasting inhibitory effect of KRH-3955 on the binding of MAb 12G5 was further tested. Molt-4 cells were preincubated with or without KRH-3955 at 10 nM. The compound was washed away, and the cells were further incubated at 37°C in compound-free growth medium. At 0, 3, and 6 h after compound removal, the cells were stained with MAb 12G5-PE and analyzed by flow cytometry. Even at 6 h after washing away of the compound, KRH-3955 inhibited MAb 12G5 binding by approximately 40% (Fig. 6b). These results suggest that KRH-3955 has a strong binding affinity for CXCR4 and a slow dissociation rate, although competition assays with the two molecules (KRH-3955 versus MAb 12G5 with radioactive, nonradioactive, or different labeling) are necessary to provide definitive conclusions.

Inhibition of MAb 12G5 binding to CXCR4 mutants by KRH-3955. The effects of different CXCR4 mutations on the inhibitory activity of KRH-3955 against MAb 12G5 binding to CXCR4 were examined. HEK293-CXCR4 transfectants were preincubated with various concentrations of KRH-3955 and AMD3100, after which the compound was washed away. The binding of PE-conjugated MAb 12G5 was measured by flow cytometry. As reported previously, AMD3100 substantially lost its blocking activity against MAb 12G5 binding for D171A (TM4), D262A (TM6), and E288A/L290A (TM7) mutants, as shown by previous reports (Table 4) (20, 37, 38). In contrast, the blocking activity of KRH-3955 against MAb 12G5 binding was not affected by the above mutations. In contrast, the H281A (ECL3) mutant displayed decreased inhibition of MAb 12G5 binding by KRH-3955 (Table 4). These data further support the hypothesis that the CXCR4 interaction sites of KRH-3955 are different from those of AMD3100.

Pharmacokinetic studies of KRH-3955 in rats. In pharmacokinetics studies, KRH-3955 was orally or intravenously administrated to Sprague-Dawley rats at a dose of 10 mg/kg. The plasma concentration of R-176211, the free form of KRH-3955, was monitored by liquid chromatography-tandem mass spectrometry. In these studies, KRH-3955 was found to be well absorbed and the absolute oral bioavailability in rats was calculated to be 25.6% based on the area under the plasma concentration-time curve (Table 5). However, KRH-3955 also showed a long elimination half-life after single-dose administration to rats, suggesting long-term accumulation of the compound in tissues (Table 5). KRH-3955 was found to be stable in human hepatic microsomes, and no significant inhibition of CYP450 liver enzymes by this compound was observed (data

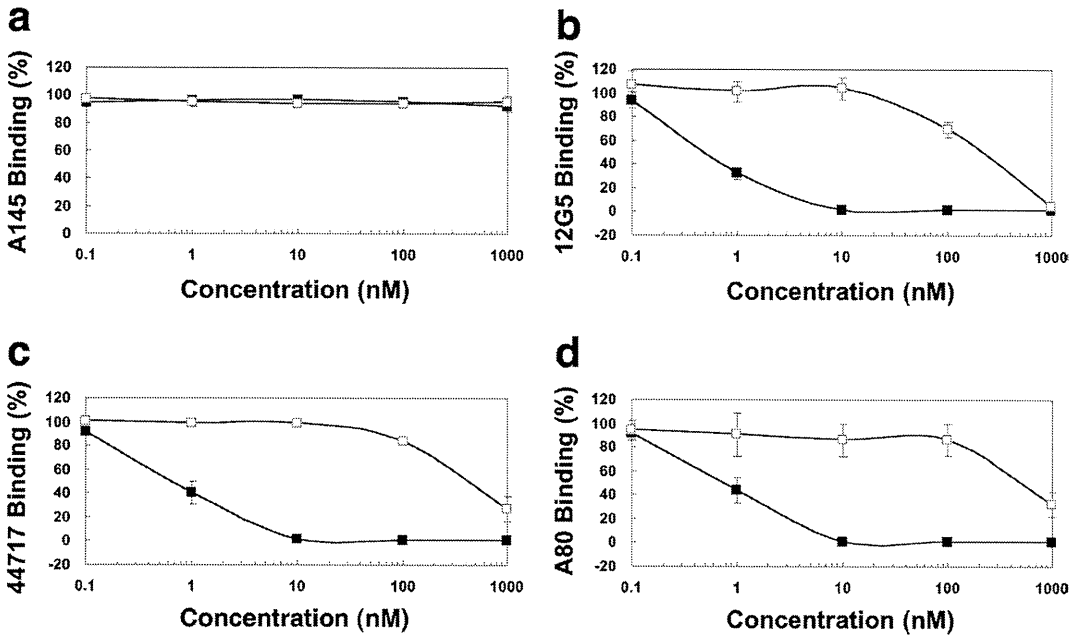

FIG. 5. Effect of KRH-3955 on the binding of four different MAbs to the CXCR4 receptor. Molt-4 cells were incubated with various concentrations of KRH-3955 (■) or AMD3100 (□). The cells were stained directly with MAbs 12G5 (recognizes ECL1 and ECL2 of CXCR4)-PE, 44717 (recognizes ECL2 of CXCR4)-PE, and A145 (recognizes the N terminus of CXCR4)-FITC or indirectly with MAb A80 (recognizes ECL3 of CXCR4). The mean fluorescence of the stained cells was analyzed with a FACScalibur flow cytometer. Percent binding was calculated with the equation described in the legend to Fig. 2. The data represent the means ± standard deviations of three independent experiments.

not shown). Thus, orally administered KRH-3955 is bioavailable in rats.

KRH-3955 efficiently suppresses X4 HIV-1 infection in hu-PBL–SCID mice. We then examined whether KRH-3955 can interfere with X4 HIV-1 infection in vivo by using hu-PBL–SCID mice. Mice were administrated a single dose (10 mg/kg) of either KRH-3955 or tartrate (as a control) p.o. and fed for 2 weeks. These mice were then engrafted with human PBMCs, and after 1 day, these "humanized" mice were infected with infectious X4 HIV-1 (NL4-3). After 7 days, human lymphocytes harvested from the peritoneal cavities and spleens of the infected mice were cultured for 4 days in vitro in the presence of rhIL-2 in order to determine the level of HIV-1 infection by the p24 enzyme-linked immunosorbent assay. The maximum concentration of KRH-3955 in blood after p.o. administration was estimated to be 100 nM (data now shown). Under these conditions, four of five mock-treated mice were infected whereas only one of five mice treated with KRH-3955 was infected (Table 6). The one infected mouse in the KRH-3955-treated group (no. 5)

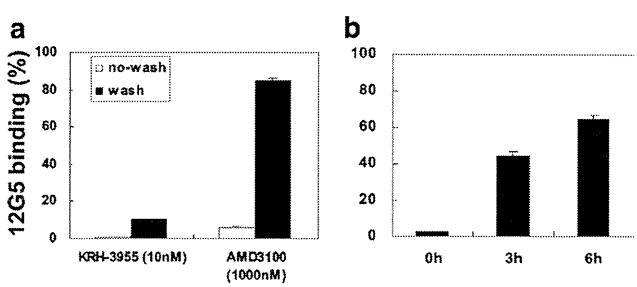

FIG. 6. Long-lasting inhibitory effects of KRH-3955 on the binding of MAb 12G5. (a) Molt-4 cells were treated with 10 nM KRH-3955 or 1,000 nM AMD3100 for 15 min. With (■) or without (□) washing, the cells were staining with MAb 12G5-PE and analyzed by flow cytometry. (b) Long-lasting inhibitory effect of KRH-3955 on the binding of MAb 12G5. Molt-4 cells were preincubated with or without KRH-3955 at 10 nM. The compound was washed away, and the cells were further incubated at 37°C in compound-free RPMI medium. At 0, 3, and 6 h after removal of the compound, the cells were staining with MAb 12G5-PE and analyzed by flow cytometry. The data represent the means of triplicate wells in a single experiment.

TABLE 4. Affinity of KRH-3955 and AMD3100 for wild-type CXCR4 and various mutant forms of CXCR4[a]

CXCR4 (location)	KRH-3955		AMD3100	
	IC_{50}	IC_{90}	IC_{50}	IC_{90}
Wild type	2.8 ± 0.5	8.2 ± 0.4	289.1 ± 25.5	971.1 ± 31.2
V99A (ECL1)	1.5 ± 0.2	7.4 ± 0.2	258.5 ± 25.9	>1,000
V112A (TM3)	2.2 ± 0.2	>10	196.6 ± 28.5	821.3 ± 15.4
H113A (TM3)	0.8 ± 0.3	6.3 ± 0.2	296.4 ± 112.2	>1,000
D171A (TM4)	3.2 ± 0.1	>10	>1,000	>1,000
D181A (ECL2)	0.5 ± 0.1	5.1 ± 0.3	143.7 ± 29.3	795.6 ± 79.9
H203A (TM5)	0.5 ± 0.1	5.3 ± 0.1	259.0 ± 11.5	860.6 ± 22.4
D262A (TM6)	1.6 ± 0.3	8.1 ± 0.5	>1,000	>1,000
E275A (ECL3)	1.0 ± 0.2	6.4 ± 0.1	235.6 ± 30.2	930.2 ± 26.1
E277A (ECL3)	3.1 ± 0.1	8.7 ± 0.1	469.5 ± 19.2	>1,000
V280A (ECL3)	1.0 ± 0.2	6.1 ± 0.1	175.3 ± 10.3	821.2 ± 47.3
H281A (ECL3)	14.1 ± 5.2	248.3 ± 74.9	72.7 ± 42.9	572.2 ± 118.1
W283A (ECL3)	1.3 ± 0.2	6.9 ± 0.2	300.2 ± 10.5	>1,000
I284A (TM7)	1.2 ± 0.2	6.8 ± 0.5	265.8 ± 20.8	>1,000
E288A/L290A (TM7)	1.6 ± 0.1	7.7 ± 0.3	>1,000	>1,000

[a] The data shown, which represent means ± SDs (n = 3) of nanomolar concentrations, were obtained from competition binding on HEK293 cells expressing the wild-type or mutant CXCR4 receptors with MAb 12G5.

TABLE 5. Pharmacokinetic parameters of KRH-3955 after single oral administration in rats[a]

Parameter	Value when given i.v. or p.o. at 10 mg/kg
Bioavailability (%)[b]	25.6
I.v. half-life (h)	99.0 ± 13.1
I.v. CL (liters/h/kg)[c]	3.9 ± 0.07
V_1 (ss) (liters/kg)[d]	374.0 ± 14
P.o. C_{max} (ng/ml)[e]	86.3 ± 23.6
T_{max} (h)[f]	2.3 ± 1.53
P.o. AUC_{0-336} (ng · h/ml)[g]	325.0 ± 38

[a] The data shown are means ± SDs (n = 3).
[b] Bioavailability = $(AUC_{oral}/AUC_{i.v.}) \times (dose_{i.v.}/dose_{oral}) \times 100$.
[c] CL, clearance.
[d] V_1 (ss), volume of distribution in central compartment at steady state.
[e] C_{max}, maximum concentration of drug in serum.
[f] T_{max}, time to maximum concentration of drug in serum.
[g] AUC_{0-336}, area under the plasma concentration-time curve from time zero to 336 h.

TABLE 6. Inhibition of infection of hu-PBL–SCID mice with X4 HIV-1 by KRH-3955[a]

Group and mouse no.	p24 produced (pg/ml)
Control	
1	747
2	10,263
3	<5
4	5,821
5	1,902
KRH-3955	
6	<5
7	<5
8	<5
9	<5
10	36

[a] Two groups of C.B-17 SCID mice (n = 5) were administrated a single dose of either KRH-3955 or tartrate (as a control) p.o. and fed for 2 weeks. These mice were then engrafted with human PBMCs (1×10^7 per animal i.p.), and after 1 day, these "humanized" mice were infected with 1,000 infective units of X4 HIV-1_{NL4-3}. IL-4 (2 mg per animal) was administrated i.p. on days 0 and 1 after PBMC engraftment to enhance X4 HIV-1 infection. After 7 days, human lymphocytes were harvested from the infected mice and cultured in vitro for 4 days in medium containing 20 U/ml IL-2. HIV-1 infection was monitored by measuring p24 levels. Means from duplicate determinations are shown. <5, below detection level.

showed low levels of p24 production. These results indicate that single-dose p.o. administration of KRH-3955 was very effective in protecting against X4 HIV-1 infection in an in vivo mouse model.

DISCUSSION

In this study, we clearly demonstrate that KRH-3955, a KRH-1636 derivative that is bioavailable when administered orally, is a potent inhibitor of HIV-1 infection both in vitro and in vivo. KRH-3955 selectively inhibited X4 HIV-1 strains, including clinical isolates, as we have previously shown with KRH-1636. Furthermore, KRH-3955 is approximately 40 times more potent than KRH-1636 in its anti-HIV-1 activity in activated PBMCs (Table 1). The anti-HIV-1 activity of KRH-3955 was independent of the PBMC donor (Table 2). KRH-3955 also inhibited the infectivity of recombinant viruses resistant to NRTIs, NNRTIs, PIs, and T20 (Table 3). Pharmacokinetic studies of KRH-3955 indicated that the compound is bioavailable in rats when administered orally (Table 5). In addition, oral administration of the compound efficiently inhibited the replication of X4 HIV-1 in the hu-PBL–SCID mouse model (Table 6). Although we could show that KRH-3955 is a potent inhibitor of subtype B HIV-1 isolates, we need to examine the efficacy of this compound against non-subtype B HIV-1 isolates because of the global nature of the HIV/AIDS epidemic and the regional diversity of HIV-1 subtypes.

R5 HIV-1 is isolated predominantly during the acute and asymptomatic stage (12) and is also believed to be important for virus transmission between individuals. In contrast, X4 HIV-1 strains emerge in approximately 50% of infected individuals and their emergence is associated with a rapid $CD4^+$ T-cell decline and disease progression (35, 50). One recent report also indicated that detection of X4 HIV-1 at baseline independently predicted disease progression (13), although it is still not known whether the emergence of X4 HIV-1 is a cause or outcome of disease progression. These findings strongly support the need for highly potent CXCR4 inhibitors that are bioavailable when administered orally such as KRH-3955.

Inhibition of ligand binding to chemokine receptors by KRH-3955 was specific for CXCR4 (Fig. 2), as we observed previously for KRH-1636. This specific inhibition of SDF-1α binding to CXCR4 by KRH-3955 is absolutely necessary for developing an anti-HIV agent to avoid immune dysregulation by nonspecific inhibition of binding by other chemokines. It is of note that the inhibitory activity of the compound against SDF-1α binding is similar to that against HIV-1 infection, which is different from that of control compound AMD3100. Where on the CXCR4 molecule is the binding site(s) of KRH-3955? Experiments to examine the effect of KRH-3955 on the binding of several anti-CXCR4 MAbs suggest that the binding sites of KRH-3955 are located in all three ECLs of CXCR4 (Fig. 5). To further define the binding site(s) of KRH-3955, we examined the effects of CXCR4 point mutations on the inhibitory activity of KRH-3955 against MAb 12G5 binding to the receptor. AMD3100 was used as a control. The inhibitory activity of AMD3100 against MAb 12G5 binding to the receptor was greatly reduced by the mutations D171A (TM4), D262A (TM6), and E288A/L290A (TM7), as reported previously (Table 4) (20, 37, 38). Of note, these mutations also affect SDF-1α binding and/or CXCR4 coreceptor activity (8). Unexpectedly, none of these three mutations affected the inhibition of MAb 12G5 binding by KRH-3955 (Table 4). Only the H281A (ECL3) mutant showed decreased inhibition of MAb 12G5 binding by KRH-3955 (Table 4). Interestingly, the same mutant modestly increased the blocking activity of AMD3100 against MAb 12G5 binding. In addition, the H281A mutation markedly impaired inhibition of MAb 12G5 binding by AMD3465, one of the prototype monocyclams (37). Further experiments with different CXCR4 mutants are necessary to identify the exact site(s) on CXCR4 targeted by this compound.

Pharmacological tests of KRH-3955 were performed with rats, and the compound was found to be bioavailable when administered orally (Table 5), which is favorable for anti-HIV drugs. However, the compound also indicated a long half-life after single-dose administration to rats, suggesting long-term accumulation of the compound in tissues, which can be either advantageous

in terms of inhibiting HIV-1 infection in hu-PBL–SCID mice (Table 6) or disadvantageous in terms of toxicity. Further studies are ongoing to determine the safety and pharmacokinetics of the compound in other animals such as dogs and monkeys. To evaluate the in vivo efficacy of KRH-3955, we used the hu-PBL–SCID mouse model and showed that oral administration of the compound strongly protected against X4 HIV-1 infection in this model system (Table 6). To achieve substantial replication of X4 HIV-1 in this system, recombinant IL-4 was added after human PBMC engraftment as described previously (23). Notably, KRH-3955 was administered only once 2 weeks before PBMC engraftment and was effective enough to block X4 HIV-1 infection, suggesting that the compound can be used as a preexposure prophylaxis agent to prevent HIV infection. This long-lasting antiviral effect of KRH-3955 can be partly explained by the strong affinity of the compound for CXCR4 (Fig. 6) and long-term accumulation of the compound in tissues.

In terms of safety of anti-HIV drugs, CCR5 antagonists are considered to be relatively safe because of the lack of obvious health problems in individuals homozygous for the CCR5 delta32 allele (27, 39). Indeed, maraviroc, a CCR5 antagonist, was approved by the U.S. FDA in 2007. In contrast, CXCR4 antagonists, which inhibit SDF-1α–CXCR4 interactions, may cause severe adverse effects because knocking out either the SDF-1α or the CXCR4 gene in mice causes marked defects such as abnormal hematopoiesis and cardiogenesis, in addition to vascularization of the gastrointestinal tract (32, 44, 52). However, no severe side effects have been reported for either AMD3100, a well-characterized CXCR4 antagonist, or AMD070, an oral CXCR4 antagonist, in human volunteers and/or HIV-infected patients. Milder side effects, including gastrointestinal symptoms and paresthesias, were common at higher doses of AMD3100. These results indicate the feasibility of using CXCR4 antagonists as anti-HIV-1 drugs in a clinical setting (21, 22, 41).

Besides the physiological roles mentioned above, the CXCR4–SDF-1 axis is also involved in various diseases such as cancer metastasis, leukemia cell progression, rheumatoid arthritis, and pulmonary fibrosis. CXCR4 antagonists such as AMD3100 and T140 have demonstrated activity in treating such CXCR4-mediated diseases (14, 46). In addition, AMD3100 is considered to be a stem cell mobilizer for transplantation in patients with cancers such as non-Hodgkin's lymphoma. Recently, AMD3100 has been shown to increase T-cell trafficking in the central nervous system, leading to significant improvement in the survival of West Nile virus encephalitis (29). Given its highly potent and selective inhibition of SDF-1–CXCR4 interaction and its bioavailability when administered orally, it is important to address whether KRH-3955 can also be used for such clinical applications.

One important issue to be addressed is whether HIV-1 strains resistant to other CXCR4 antagonists show cross-resistance to KRH-3955. In our preliminary studies, AMD3100-resistant HIV-1 (kindly provided by M. Baba, Kagoshima University) (4) showed ~19-fold resistance to KRH-3955 compared with parental NL4-3, whereas the resistant virus showed ~40-fold resistance to both AMD3100 and AMD070 in MT-4 cells (data not shown). Interestingly, the AMD3100-resistant HIV-1 strain was relatively sensitive to T22, another prototype CXCR4 antagonist. Thus, KRH-3955 target sites on CXCR4 seem to partially overlap those of AMD3100, although experiments with CXCR4 mutants do not support this idea. It is important to establish KRH-3955-resistant mutants and investigate whether they also show cross-resistance to other CXCR4 antagonists. Long-term culture experiments with PM1/CCR5 cells that express both CXCR4 and CCR5 infected with X4 HIV-1 in the presence of KRH-3955 are in progress.

In conclusion, KRH-3955 is a small-molecule antagonist of the CXCR4 receptor that is bioavailable when administered orally. The compound potently and selectively inhibits X4 HIV-1 infection both in vitro and in vivo. Thus, KRH-3955 is a promising antiviral agent for HIV-1 infection and should be evaluated for its clinical efficacy and safety in humans.

ACKNOWLEDGMENTS

We thank E. Freed for his critical review of the manuscript. We thank Y. Koyanagi, and R. Collman for generously providing plasmids and thank M. Baba for AMD3100-resistant HIV-1.

The following reagents were obtained from the NIH AIDS Research and Reference Reagent Program: saquinavir, subtype B HIV-1 primary isolates 92HT593, 92HT599 (N. Hasley), and 91US005 (B. Hahn) and AZT-resistant HIV-1 A018 (D. Richman). This work was supported in part by a grant for Research on HIV/AIDS from the Ministry of Health, Labor, and Welfare of Japan.

REFERENCES

1. **Adachi, A., H. E. Gendelman, S. Koenig, T. Folks, R. Willey, A. Rabson, and M. A. Martin.** 1986. Production of acquired immunodeficiency syndrome-associated retrovirus in human and nonhuman cells transfected with an infectious molecular clone. J. Virol. **59**:284–291.
2. **Alkhatib, G., C. Combadiere, C. C. Broder, Y. Feng, P. E. Kennedy, P. M. Murphy, and E. A. Berger.** 1996. CC CKR5: a RANTES, MIP-1α, MIP-1β receptor as a fusion cofactor for macrophage-tropic HIV-1. Science **272**:1955–1958.
3. **Amara, A., S. L. Gall, O. Schwartz, J. Salamero, M. Montes, P. Loetscher, M. Baggiolini, J. L. Virelizier, and F. Arenzana-Seisdedos.** 1997. HIV coreceptor downregulation as antiviral principle: SDF-1α-dependent internalization of the chemokine receptor CXCR4 contributes to inhibition of HIV replication. J. Exp. Med. **186**:139–146.
4. **Arakaki, R., H. Tamamura, M. Premanathan, K. Kanbara, S. Ramanan, K. Mochizuki, M. Baba, N. Fujii, and H. Nakashima.** 1999. T134, a small-molecule CXCR4 inhibitor, has no cross-drug resistance with AMD3100, a CXCR4 antagonist with a different structure. J. Virol. **73**:1719–1723.
5. **Baba, M., O. Nishimura, N. Kanzaki, M. Okamoto, H. Sawada, Y. Iizawa, M. Shiraishi, Y. Aramaki, K. Okonogi, Y. Ogawa, K. Meguro, and M. Fujino.** 1999. A small-molecule, nonpeptide CCR5 antagonist with highly potent and selective anti-HIV-1 activity. Proc. Natl. Acad. Sci. USA **96**:5698–5703.
6. **Baba, M., K. Takashima, H. Miyake, N. Kanzaki, K. Teshima, X. Wang, M. Shiraishi, and Y. Iizawa.** 2005. TAK-652 inhibits CCR5-mediated human immunodeficiency virus type 1 infection in vitro and has favorable pharmacokinetics in humans. Antimicrob. Agents Chemother. **49**:4584–4591.
7. **Bleul, C. C., M. Farzan, H. Choe, C. Parolin, I. Clark-Lewis, J. Sodroski, and T. A. Springer.** 1996. The lymphocyte chemoattractant SDF-1 is a ligand for LESTR/fusin and blocks HIV-1 entry. Nature **382**:829–833.
8. **Brelot, A., N. Heveker, M. Montes, and M. Alizon.** 2000. Identification of residues of CXCR4 critical for human immunodeficiency virus coreceptor and chemokine receptor activities. J. Biol. Chem. **275**:23736–23744.
9. **Coakley, E., C. J. Petropoulos, and J. M. Whitcomb.** 2005. Assessing chemokine co-receptor usage in HIV. Curr. Opin. Infect. Dis. **18**:9–15.
10. **Cocchi, F., A. L. DeVico, D. A. Garzino, S. K. Arya, R. C. Gallo, and P. Lusso.** 1995. Identification of RANTES, MIP-1α, and MIP-1β as the major HIV-suppressive factors produced by $CD8^+$ T cells. Science **270**:1811–1815.
11. **Collman, R., J. W. Balliet, S. A. Gregory, H. Friedman, D. L. Kolson, N. Nathanson, and A. Srinivasan.** 1992. An infectious molecular clone of an unusual macrophage-tropic and highly cytopathic strain of human immunodeficiency virus type 1. J. Virol. **66**:7517–7521.
12. **Connor, R. I., K. E. Sheridan, D. Ceradini, S. Choe, and N. R. Landau.** 1997. Change in coreceptor use correlates with disease progression in HIV-1-infected individuals. J. Exp. Med. **185**:621–628.
13. **Daar, E. S., K. L. Kesler, C. J. Petropoulos, W. Huang, M. Bates, A. E. Lail, E. P. Coakley, E. D. Gomperts, and S. M. Donfield.** 2007. Baseline HIV type 1 coreceptor tropism predicts disease progression. Clin. Infect. Dis. **45**:643–649.
14. **De Clercq, E.** 2005. Potential clinical applications of the CXCR4 antagonist bicyclam AMD3100. Mini Rev. Med. Chem. **5**:805–824.
15. **Deng, H., R. Liu, W. Ellmeier, S. Choe, D. Unutmaz, M. Burkhart, M. P. Di, S. Marmon, R. E. Sutton, C. M. Hill, C. B. Davis, S. C. Peiper, T. J. Schall, D. R. Littman, and N. R. Landau.** 1996. Identification of a major co-receptor for primary isolates of HIV-1. Nature **381**:661–666.

16. **Donzella, G. A., D. Schols, S. W. Lin, J. A. Este, K. A. Nagashima, P. J. Maddon, G. P. Allaway, T. P. Sakmar, G. Henson, E. De Clercq, and J. P. Moore.** 1998. AMD3100, a small molecule inhibitor of HIV-1 entry via the CXCR4 co-receptor. Nat. Med. **4:**72–77.
17. **Dorr, P., M. Westby, S. Dobbs, P. Griffin, B. Irvine, M. Macartney, J. Mori, G. Rickett, C. Smith-Burchnell, C. Napier, R. Webster, D. Armour, D. Price, B. Stammen, A. Wood, and M. Perros.** 2005. Maraviroc (UK-427,857), a potent, orally bioavailable, and selective small-molecule inhibitor of chemokine receptor CCR5 with broad-spectrum anti-human immunodeficiency virus type 1 activity. Antimicrob. Agents Chemother. **49:**4721–4732.
18. **Dragic, T., V. Litwin, G. P. Allaway, S. R. Martin, Y. Huang, K. A. Nagashima, C. Cayanan, P. J. Maddon, R. A. Koup, J. P. Moore, and W. A. Paxton.** 1996. HIV-1 entry into $CD4^+$ cells is mediated by the chemokine receptor CC-CKR-5. Nature **381:**667–673.
19. **Feng, Y., C. C. Broder, P. E. Kennedy, and E. A. Berger.** 1996. HIV-1 entry cofactor: functional cDNA cloning of a seven-transmembrane, G protein-coupled receptor. Science **272:**872–877.
20. **Gerlach, L. O., R. T. Skerlj, G. J. Bridger, and T. W. Schwartz.** 2001. Molecular interactions of cyclam and bicyclam non-peptide antagonists with the CXCR4 chemokine receptor. J. Biol. Chem. **276:**14153–14160.
21. **Hendrix, C. W., A. C. Collier, M. M. Lederman, D. Schols, R. B. Pollard, S. Brown, J. B. Jackson, R. W. Coombs, M. J. Glesby, C. W. Flexner, G. J. Bridger, K. Badel, R. T. MacFarland, G. W. Henson, and G. Calandra.** 2004. Safety, pharmacokinetics, and antiviral activity of AMD3100, a selective CXCR4 receptor inhibitor, in HIV-1 infection. J. Acquir. Immune Defic. Syndr. **37:**1253–1262.
22. **Hendrix, C. W., C. Flexner, R. T. MacFarland, C. Giandomenico, E. J. Fuchs, E. Redpath, G. Bridger, and G. W. Henson.** 2000. Pharmacokinetics and safety of AMD-3100, a novel antagonist of the CXCR-4 chemokine receptor, in human volunteers. Antimicrob. Agents Chemother. **44:**1667–1673.
23. **Ichiyama, K., S. Yokoyama-Kumakura, Y. Tanaka, R. Tanaka, K. Hirose, K. Bannai, T. Edamatsu, M. Yanaka, Y. Niitani, N. Miyano-Kurosaki, H. Takaku, Y. Koyanagi, and N. Yamamoto.** 2003. A duodenally absorbable CXC chemokine receptor 4 antagonist, KRH-1636, exhibits a potent and selective anti-HIV-1 activity. Proc. Natl. Acad. Sci. USA **100:**4185–4190.
24. **Kikukawa, R., Y. Koyanagi, S. Harada, N. Kobayashi, M. Hatanaka, and N. Yamamoto.** 1986. Differential susceptibility to the acquired immunodeficiency syndrome retrovirus in cloned cells of human leukemic T-cell line Molt-4. J. Virol. **57:**1159–1162.
25. **Koyanagi, Y., S. Miles, R. T. Mitsuyasu, J. E. Merrill, H. V. Vinters, and I. S. Chen.** 1987. Dual infection of the central nervous system by AIDS viruses with distinct cellular tropisms. Science **236:**819–822.
26. **Larder, B. A., G. Darby, and D. D. Richman.** 1989. HIV with reduced sensitivity to zidovudine (AZT) isolated during prolonged therapy. Science **243:**1731–1734.
27. **Liu, R., W. A. Paxton, S. Choe, D. Ceradini, S. R. Martin, R. Horuk, M. E. MacDonald, H. Stuhlmann, R. A. Koup, and N. R. Landau.** 1996. Homozygous defect in HIV-1 coreceptor accounts for resistance of some multiply-exposed individuals to HIV-1 infection. Cell **86:**367–377.
28. **Maeda, K., H. Nakata, Y. Koh, T. Miyakawa, H. Ogata, Y. Takaoka, S. Shibayama, K. Sagawa, D. Fukushima, J. Moravek, Y. Koyanagi, and H. Mitsuya.** 2004. Spirodiketopiperazine-based CCR5 inhibitor which preserves CC-chemokine/CCR5 interactions and exerts potent activity against R5 human immunodeficiency virus type 1 in vitro. J. Virol. **78:**8654–8662.
29. **McCandless, E. E., B. Zhang, M. S. Diamond, and R. S. Klein.** 2008. CXCR4 antagonism increases T cell trafficking in the central nervous system and improves survival from West Nile virus encephalitis. Proc. Natl. Acad. Sci. USA **105:**11270–11275.
30. **Murakami, T., T. Nakajima, Y. Koyanagi, K. Tachibana, N. Fujii, H. Tamamura, N. Yoshida, M. Waki, A. Matsumoto, O. Yoshie, T. Kishimoto, N. Yamamoto, and T. Nagasawa.** 1997. A small molecule CXCR4 inhibitor that blocks T cell line-tropic HIV-1 infection. J. Exp. Med. **186:**1389–1393.
31. **Murakami, T., T. Y. Zhang, Y. Koyanagi, Y. Tanaka, J. Kim, Y. Suzuki, S. Minoguchi, H. Tamamura, M. Waki, A. Matsumoto, N. Fujii, H. Shida, J. A. Hoxie, S. C. Peiper, and N. Yamamoto.** 1999. Inhibitory mechanism of the CXCR4 antagonist T22 against human immunodeficiency virus type 1 infection. J. Virol. **73:**7489–7496.
32. **Nagasawa, T., S. Hirota, K. Tachibana, N. Takakura, S. Nishikawa, Y. Kitamura, N. Yoshida, H. Kikutani, and T. Kishimoto.** 1996. Defects of B-cell lymphopoiesis and bone-marrow myelopoiesis in mice lacking the CXC chemokine PBSF/SDF-1. Nature **382:**635–638.
33. **Nakashima, H., M. Masuda, T. Murakami, Y. Koyanagi, A. Matsumoto, N. Fujii, and N. Yamamoto.** 1992. Anti-human immunodeficiency virus activity of a novel synthetic peptide, T22 ([Tyr-5,12, Lys-7]polyphemusin II): a possible inhibitor of virus-cell fusion. Antimicrob. Agents Chemother. **36:**1249–1255.
34. **Oberlin, E., A. Amara, F. Bachelerie, C. Bessia, J. L. Virelizier, F. Arenzana-Seisdedos, O. Schwartz, J. M. Heard, I. Clark-Lewis, D. F. Legler, M. Loetscher, M. Baggiolini, and B. Moser.** 1996. The CXC chemokine SDF-1 is the ligand for LESTR/fusin and prevents infection by T-cell-line-adapted HIV-1. Nature **382:**833–835.
35. **Richman, D. D., and S. A. Bozzette.** 1994. The impact of the syncytium-inducing phenotype of human immunodeficiency virus on disease progression. J. Infect. Dis. **169:**968–974.
36. **Roehm, N. W., G. H. Rodgers, S. M. Hatfield, and A. L. Glasebrook.** 1991. An improved colorimetric assay for cell proliferation and viability utilizing the tetrazolium salt XTT. J. Immunol. Methods **142:**257–265.
37. **Rosenkilde, M. M., L. O. Gerlach, S. Hatse, R. T. Skerlj, D. Schols, G. J. Bridger, and T. W. Schwartz.** 2007. Molecular mechanism of action of monocyclam versus bicyclam non-peptide antagonists in the CXCR4 chemokine receptor. J. Biol. Chem. **282:**27354–27365.
38. **Rosenkilde, M. M., L. O. Gerlach, J. S. Jakobsen, R. T. Skerlj, G. J. Bridger, and T. W. Schwartz.** 2004. Molecular mechanism of AMD3100 antagonism in the CXCR4 receptor: transfer of binding site to the CXCR3 receptor. J. Biol. Chem. **279:**3033–3041.
39. **Samson, M., F. Libert, B. J. Doranz, J. Rucker, C. Liesnard, C. M. Farber, S. Saragosti, C. Lapoumeroulie, J. Cognaux, C. Forceille, G. Muyldermans, C. Verhofstede, G. Burtonboy, M. Georges, T. Imai, S. Rana, Y. Yi, R. J. Smyth, R. G. Collman, R. W. Doms, G. Vassart, and M. Parmentier.** 1996. Resistance to HIV-1 infection in Caucasian individuals bearing mutant alleles of the CCR-5 chemokine receptor gene. Nature **382:**722–725.
40. **Schols, D., S. Struyf, J. Van Damme, J. A. Este, G. Henson, and E. De Clercq.** 1997. Inhibition of T-tropic HIV strains by selective antagonization of the chemokine receptor CXCR4. J. Exp. Med. **186:**1383–1388.
41. **Stone, N. D., S. B. Dunaway, C. Flexner, C. Tierney, G. B. Calandra, S. Becker, Y. J. Cao, I. P. Wiggins, J. Conley, R. T. MacFarland, J. G. Park, C. Lalama, S. Snyder, B. Kallungal, K. L. Klingman, and C. W. Hendrix.** 2007. Multiple-dose escalation study of the safety, pharmacokinetics, and biologic activity of oral AMD070, a selective CXCR4 receptor inhibitor, in human subjects. Antimicrob. Agents Chemother. **51:**2351–2358.
42. **Strizki, J. M., C. Tremblay, S. Xu, L. Wojcik, N. Wagner, W. Gonsiorek, R. W. Hipkin, C. C. Chou, C. Pugliese-Sivo, Y. Xiao, J. R. Tagat, K. Cox, T. Priestley, S. Sorota, W. Huang, M. Hirsch, G. R. Reyes, and B. M. Baroudy.** 2005. Discovery and characterization of vicriviroc (SCH 417690), a CCR5 antagonist with potent activity against human immunodeficiency virus type 1. Antimicrob. Agents Chemother. **49:**4911–4919.
43. **Strizki, J. M., S. Xu, N. E. Wagner, L. Wojcik, J. Liu, Y. Hou, M. Endres, A. Palani, S. Shapiro, J. W. Clader, W. J. Greenlee, J. R. Tagat, S. McCombie, K. Cox, A. B. Fawzi, C. C. Chou, C. Pugliese-Sivo, L. Davies, M. E. Moreno, D. D. Ho, A. Trkola, C. A. Stoddart, J. P. Moore, G. R. Reyes, and B. M. Baroudy.** 2001. SCH-C (SCH 351125), an orally bioavailable, small molecule antagonist of the chemokine receptor CCR5, is a potent inhibitor of HIV-1 infection in vitro and in vivo. Proc. Natl. Acad. Sci. USA **98:**12718–12723.
44. **Tachibana, K., S. Hirota, H. Iizasa, H. Yoshida, K. Kawabata, Y. Kataoka, Y. Kitamura, K. Matsushima, N. Yoshida, S. Nishikawa, T. Kishimoto, and T. Nagasawa.** 1998. The chemokine receptor CXCR4 is essential for vascularization of the gastrointestinal tract. Nature **393:**591–594.
45. **Takashima, K., H. Miyake, N. Kanzaki, Y. Tagawa, X. Wang, Y. Sugihara, Y. Iizawa, and M. Baba.** 2005. Highly potent inhibition of human immunodeficiency virus type 1 replication by TAK-220, an orally bioavailable small-molecule CCR5 antagonist. Antimicrob. Agents Chemother. **49:**3474–3482.
46. **Tamamura, H., H. Tsutsumi, H. Masuno, and N. Fujii.** 2007. Development of low molecular weight CXCR4 antagonists by exploratory structural tuning of cyclic tetra- and pentapeptide-scaffolds towards the treatment of HIV infection, cancer metastasis and rheumatoid arthritis. Curr. Med. Chem. **14:**93–102.
47. **Tanaka, R., A. Yoshida, T. Murakami, E. Baba, J. Lichtenfeld, T. Omori, T. Kimura, N. Tsurutani, N. Fujii, Z. X. Wang, S. C. Peiper, N. Yamamoto, and Y. Tanaka.** 2001. Unique monoclonal antibody recognizing the third extracellular loop of CXCR4 induces lymphocyte agglutination and enhances human immunodeficiency virus type 1-mediated syncytium formation and productive infection. J. Virol. **75:**11534–11543.
48. **Urano, E., T. Aoki, Y. Futahashi, T. Murakami, Y. Morikawa, N. Yamamoto, and J. Komano.** 2008. Substitution of the myristoylation signal of human immunodeficiency virus type 1 $Pr55^{Gag}$ with the phospholipase C-δ1 pleckstrin homology domain results in infectious pseudovirion production. J. Gen. Virol. **89:**3144–3149.
49. **Westby, M., M. Lewis, J. Whitcomb, M. Youle, A. L. Pozniak, I. T. James, T. M. Jenkins, M. Perros, and E. van der Ryst.** 2006. Emergence of CXCR4-using human immunodeficiency virus type 1 (HIV-1) variants in a minority of HIV-1-infected patients following treatment with the CCR5 antagonist maraviroc is from a pre-treatment CXCR4-using virus reservoir. J. Virol. **80:**4909–4920.
50. **Xiao, L., D. L. Rudolph, S. M. Owen, T. J. Spira, and R. B. Lal.** 1998. Adaptation to promiscuous usage of CC and CXC-chemokine coreceptors in vivo correlates with HIV-1 disease progression. AIDS **12:**F137–F143.
51. **Yoshida, A., R. Tanaka, T. Murakami, Y. Takahashi, Y. Koyanagi, M. Nakamura, M. Ito, N. Yamamoto, and Y. Tanaka.** 2003. Induction of protective immune responses against R5 human immunodeficiency virus type 1 (HIV-1) infection in hu-PBL–SCID mice by intrasplenic immunization with HIV-1-pulsed dendritic cells: possible involvement of a novel factor of human $CD4^+$ T-cell origin. J. Virol. **77:**8719–8728.
52. **Zou, Y. R., A. H. Kottmann, M. Kuroda, I. Taniuchi, and D. R. Littman.** 1998. Function of the chemokine receptor CXCR4 in haematopoiesis and in cerebellar development. Nature **393:**595–599.

Efficient inhibition of SDF-1α-mediated chemotaxis and HIV-1 infection by novel CXCR4 antagonists

Yuki Iwasaki,[1] Hirofumi Akari,[1,4] Tsutomu Murakami,[2] Sei Kumakura,[3] Md. Zahidunnabi Dewan,[2,5] Mikiro Yanaka[3,6] and Naoki Yamamoto[2]

[1]Laboratory of Disease Control, Tsukuba Primate Research Center, National Institute of Biomedical Innovation, Tsukuba; [2]AIDS Research Center, National Institute of Infectious Diseases, Tokyo; [3]Biomedical Research Laboratories, Kureha Corporation, Tokyo, Japan

(Received November 11, 2008/Revised December 25, 2008/Accepted December 25, 2008/Online publication February 24, 2009)

CXC chemokine receptor-4, the receptor for stromal cell-derived factor-1α as well as human immunodeficiency virus type 1, belongs to the chemokine receptor family and has been shown to play a critical role in directing the migration of cancer cells to sites of metastasis as well as human immunodeficiency virus type 1 infection. We had previously reported that a duodenally absorbable CXC chemokine receptor-4 antagonist, KRH-1636, showed a potent anti-human immunodeficiency virus type 1 activity both *in vivo* and *in vitro*. In this study, we initially examined the effect of the compound and its derivatives on stromal cell-derived factor-1α-mediated chemotaxis of cancer cells in order to evaluate if they could be applicable as a novel inhibitor of cancer metastasis. We found that both KRH-2731 and KRH-3955 were highly potent antagonists of stromal cell-derived factor-1α-mediated chemotaxis, i.e. the derivatives exhibited 50% effective concentrations of less than 10 nM, for more than 1000-fold efficacy improvement over the prototype KRH-1636. We further demonstrated the greater anti-human immunodeficiency virus type 1 efficacy of the derivatives compared with the original KRH-1636. Taken together, the KRH-1636 derivatives KRH-2731 and KRH-3955 may be promising as a novel inhibitory drug for cancer metastasis as well as for human immunodeficiency virus type 1 infection. (*Cancer Sci* 2009; 100: 778–781)

Chemokines are secretory proteins with a molecular weight of about 8–14 kDa, and are generally alkaline and heparin-bound. The small chemokine proteins are classified into four highly conserved groups, i.e. CXC, CC, C, and CX3C (X indicates the number of amino acids between the cysteine residues) on the basis of the position of the first two cysteines that are adjacent to the amino terminus.[1] An established role for several members of the CXC and CC chemokine families is to provide directional cues for the movement of leukocytes in development, homeostasis, and inflammation.[2] At the time of the movement of leukocytes, chemokine concentration gradually increases at the inflammatory site because the chemoattractants released from the luminal surface of the endothelium, the inflammatory site of the lymphocyte, are rapidly diluted and swept downstream by blood flow. Leukocytes in the mainstream of blood flow may make contact with the endothelium via a group of molecules called selectins,[3] and may then roll along the endothelial surface.

The cell surface molecule CXC chemokine receptor-4 (CXCR4) is a 7-transmembrane-spanning, G-protein-coupled receptor for the CXC chemokine stromal cell-derived factor-1α (SDF-1α)/pre-B-cell growth stimulating factor (PBSF)/CXCL12.[2] The open reading frame of the *CXCR4* gene encodes a peptide of 352 amino acids and is interrupted by one intron in the region encoding the N-terminal segment.[4]

CXCR4 is a receptor for the SDF-1α. SDF-1α interacts with CXCR4 to play a variety of physiological roles: B-cell formation in liver and bone marrow at the fetal stage, homing of bone marrow cells in the developmental process, formation of the interventricular septum, regulation of movement of the cerebellum granule cell in neurogenesis, and large vasculogenesis that nourishes the gastrointestinal tract.[2] Since both CXCR4 and SDF-1α knockout mice do not survive, the interaction between these molecules is essential in the developmental process.[5–7] It has been reported recently that CXCR7 binds with high affinity to SDF-1α and to interferon-inducible T-cell α-chemoattractant (I-TAC, also known as CXCL11).[8] However, unlike other chemokine receptors, ligand activation of CXCR7 induces neither Ca^{2+} mobilization nor cell migration.[8]

CXCR4 is also shown to be one of the coreceptors for human immunodeficiency virus type 1 (HIV-1).[9] Entry of HIV-1 into target cells involves interactions of the viral envelope protein (Env) with CD4 and a coreceptor, mainly either CXCR4 for T-cell–tropic HIV-1,[10,11] or CCR5 for macrophage–tropic HIV-1.[12,13] In acute HIV-1 infection, primarily macrophage-tropic strains are involved in transmission of the virus, whereas T-cell–tropic strains emerge later and are associated with the rapid progression to AIDS.[9]

Importantly, cancer cells originating from the pancreas, brain, breast, prostate, kidney, ovaries, thyroid, and malignant melanoma express CXCR4; however, normal tissues scarcely express CXCR4. Increasing CXCR4 promotes metastasis of these tumor cells toward SDF-1α-expressing organs including the lungs, liver, lymph nodes, bone marrow, and adrenal glands.[14–17] Further, interaction between CXCR4 and SDF-1α promotes progression of chronic and acute lymphocytic leukemia,[3] and exacerbation of chronic rheumatoid arthritis.[18]

We previously reported that a duodenally absorbable CXCR4 antagonist, KRH-1636, competitively blocked the association of the Env protein of HIV-1 with CXCR4 both *in vivo* and *in vitro* as well as the interaction of SDF-1α with CXCR4.[19] We therefore hypothesized that KRH-1636 could be a promising chemical for offering protection from both cancer metastases induced by SDF-1α and from CXCR4-tropic HIV-1 infection. In order to assess this possibility, we sought to evaluate whether the CXCR4 antagonist KRH-1636 and its derivatives could potently inhibit SDF-1α-mediated chemotaxis of cancer cells as well as HIV-1 infection.

Materials and Methods

Reagents. SDF-1α (R&D systems, Minneapolis, MN, USA) was dissolved in phosphate-buffered saline (PBS) at 1 μM. KRH-1636,[19] and its derivatives KRH-2731, -3148, and -3955 were synthesized at Kureha Chemical Industry (Tokyo, Japan). These

[4]To whom correspondence should be addressed. E-mail: akari@nibio.go.jp
[5]Current address: Department of Pathology, New York University School of Medicine, 550 First Avenue, New York, NY 10016, USA
[6]Current address: Kureha Special Laboratory Co. Ltd. Fukushima 974-8232, Japan
Abbreviations: CXCR4, CXC chemokine receptor-4; DMSO, dimetyl sulfoxide; EC_{50}, 50% effective concentration; Env, envelope protein; FACS, fluorescence-activated cell sorter; FCS, fetal calf serum; HIV-1, human immunodeficiency virus type 1; mAb, monoclonal antibody; OD, optical density; PBS, phosphate-buffered saline; PBSF, pre-B-cell growth stimulating factor; PE, phycoerythrin; SDF-1α, stromal cell derived factor-1α.

doi: 10.1111/j.1349-7006.2009.01104.x

compounds were dissolved in dimethyl sulfoxide (DMSO) at a final concentration of 0.1%.

Cell culture. Jurkat and its subline Jurkat E6-1 were used in this study. The cells were cultured in a complete medium (CM) composed of RPMI-1640 (Sigma, Tokyo, Japan) supplemented with 10% fetal calf serum (FCS), 100 U/mL penicillin, 100 μg/mL streptomycin, and 0.1% 2-Mercaptoethanol at 37°C in a humidified environment with a 5% CO_2 atmosphere.

Fluorescence-activated cell sorter (FACS) analysis. Expression of CXCR4 and CD4 on Jurkat cells was measured by flow cytometry. The cells were suspended at 1×10^5 cells/mL in PBS containing 1% FCS. The cells were reacted with phycoerythrin (PE)-labeled mouse monoclonal antibodies (mAbs) to human CXCR4 (12G5; eBioscience, San Diego, USA) and CD4 (Leu3a; Becton Dickinson, Tokyo, Japan) as a positive control at 4°C for 1 h. The treated cells were washed and fixed with 1% formalin in PBS. Fluorescence of the stained cells was detected by a FACSCalibur (Becton Dickinson), followed by the analysis of fluorescence intensity by CellQuest software (Becton Dickinson).

Cytotoxic assay. Jurkat cells were treated with CXCR4 antagonists at 37°C for 1 h. The cells were harvested and resuspended in a 96-well plate. The viability of the treated cells was measured using a Cell Counting Kit-8 (Dojindo, Tokyo, Japan).

Chemotaxis assay. Cellular chemotaxis was investigated using a 24-well culture plate with 8-μm-pore filters (Transwell; Corning, Tokyo, Japan). Jurkat cells were washed three times in a FCS-free medium and suspended at 3×10^6 cells/mL in RPMI-1640 containing 0.1% bovine serum albumin (control medium). The control medium (0.2 mL) containing 3×10^5 cells was added to the upper well; the control medium (0.6 mL) with or without SDF-1α (100 ng/mL) or CXCR4 antagonists (10 μM) was added to the lower well. The culture plate was incubated for 3 h at 37°C; thereafter, the cells in the upper or lower well were then harvested and resuspended in a 96-well plate. The number of cells in each well was measured using a Cell Counting Kit-8. Optical density (OD) (455 nm/650 nm) values were measured on a microplate reader. The chemotaxis index was calculated as follows: [(OD of treated cells in the lower well – OD of control medium in the lower well)/(OD in sum of the lower and upper wells – OD of control medium in the lower well)] × 100.

For evaluating the inhibitory effect of the CXCR4 antagonists on chemotaxis, cells were pretreated with CXCR4 antagonists at 37°C for 1 h, followed by the chemotaxis assay as stated above.

Anti-HIV-1 assay. Human peripheral blood mononuclear cells, which were activated with immobilized anti-CD3 mouse mAb in RPMI-1640 medium supplemented with 10% FCS for 3 days, were infected with NL4-3 at a multiplicity of infection of 0.001. After 3 h of adsorption, the cells were washed, and cultured in CM supplemented with recombinant human interleukin-2 (50 U/mL), in the presence or absence of the test compounds. Amounts of HIV-1 capsid (p24) antigen produced in the culture supernatants were measured by an enzyme-linked immunosorbent assay kit (ZeptoMetrix Corp., Buffalo, NY, USA) 7–10 days after infection.

Results

The initial purpose of this study was to evaluate whether a series of CXCR4 antagonists could inhibit cancer metastasis, which is promoted by the interaction between SDF-1α and CXCR4. In order to evaluate the antagonistic effect of the compounds, we sought to develop an assay system for quantitatively detecting SDF-1α-mediated chemotaxis induced by the interaction. In this experiment, we employed $CD4^+$ leukemic cell line Jurkat as a $CXCR4^+$ indicator.[20] Since Jurkat sublines have different characteristics, we compared CXCR4 expression in the original Jurkat cells and its subline E6-1 by using flow cytometry. As expected, CXCR4 expression was comparable in both cell lines, while CD4 expression was greater in the Jurkat cells (Fig. 1a).

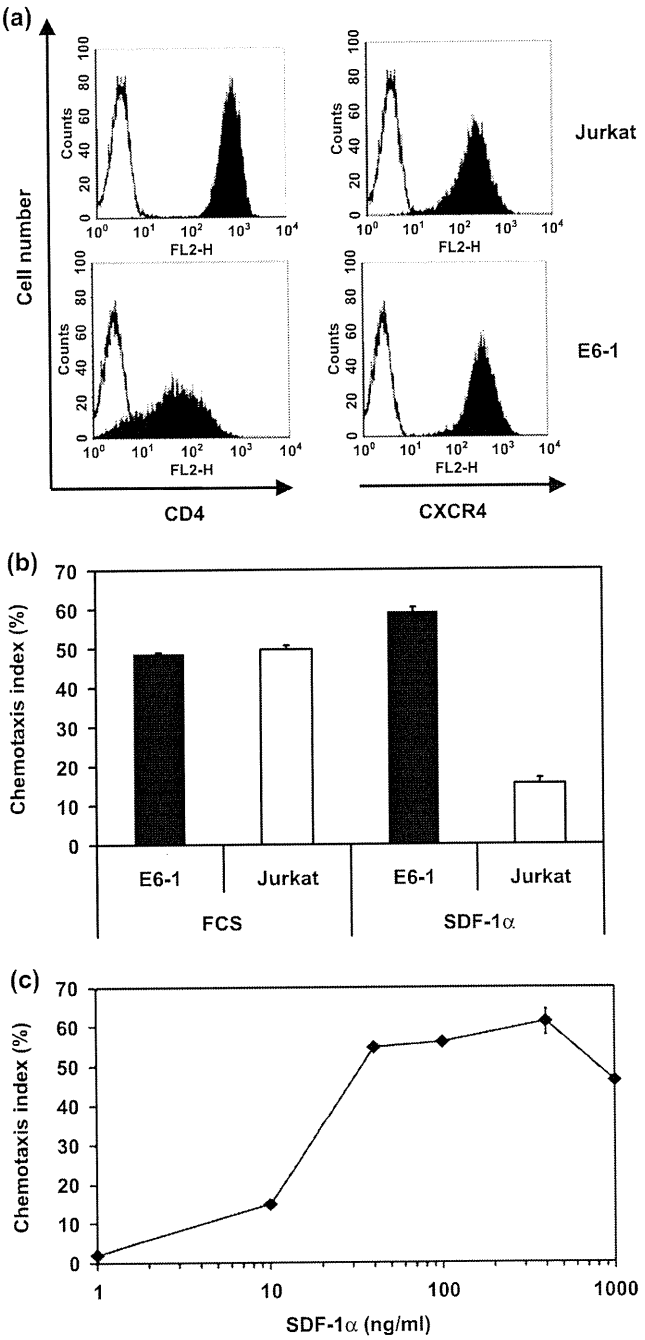

Fig. 1. A quantitative assay system for stromal cell-derived factor-1α (SDF-1α)-mediated chemotaxis. (a) Evaluation of CD4 and CXC chemokine receptor-4 (CXCR4) expression on Jurkat and its subline E6-1. The cells were stained with phycoerythrin-labeled anti-CXCR4 or anti-CD4 mouse monoclonal antibodies. Open and closed lines indicate fluorescence of the control and stained cells, respectively. (b) Effect of SDF-1α on chemotaxis of Jurkat and its subline E6-1. The cell lines were incubated with the control medium including 400 ng/mL of SDF-1α or 10% fetal calf serum (FCS) for 24 h at 37°C. The results are shown as a chemotaxis index and standard deviation. The calculation of the chemotaxis index is described in 'Materials and Methods'. (c) Dose-dependent effect of SDF-1α on the chemotaxis of E6-1 cells. Increasing amounts of SDF-1α were treated with E6-1 cells for 3 h and the levels of migration to the lower well are indicated as a chemotaxis index.

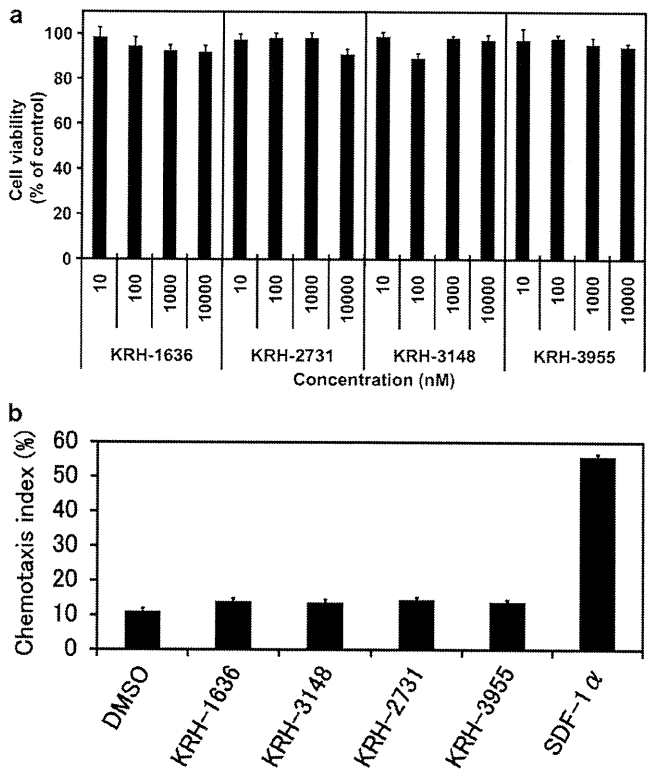

Fig. 2. CXC chemokine receptor-4 (CXCR4) antagonists exhibited neither cytotoxic nor agonistic effects. (a) Increasing amounts of CXCR4 antagonists were examined for their cytotoxic effect on E6-1 cells. (b) CXCR4 antagonists (10 μM) or stromal cell-derived factor-1α (SDF-1α) (100 ng/mL) were added to the lower wells in a chemotaxis assay and were incubated at 37°C for 3 h. The treated E6-1 cells were evaluated for the chemotaxis index. DMSO, dimethyl sulfoxide.

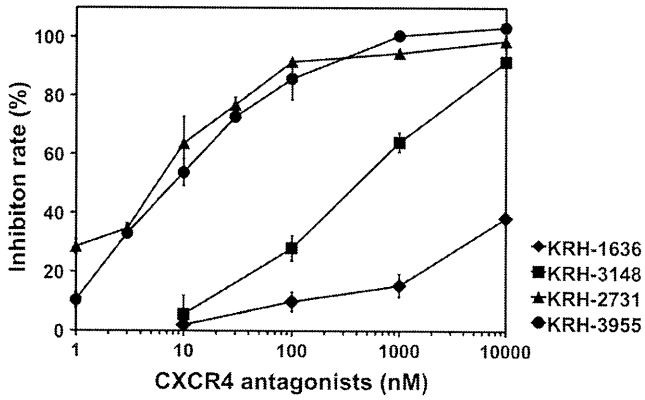

Fig. 3. Dose-dependent effect of CXC chemokine receptor-4 (CXCR4) antagonists on inhibition of stromal cell-derived factor-1α (SDF-1α)-mediated chemotaxis. E6-1 cells were pretreated with each concentration of CXCR4 antagonists at 37°C for 1 h, followed by incubation with 100 ng/mL of SDF-1α for 3 h. The cells were evaluated for the chemotaxis index. The inhibition rate was calculated as the percentage inhibition of chemotaxis by the antagonists.

Table 1. Inhibitory effects of CXCR4 antagonists on SDF-1α-mediated chemotaxis and HIV-1 infection

CXCR4 antagonists	CXCR4 (EC_{50}, nM)	
	Chemotaxis	HIV-1
KRH-1636	>10 000	42
KRH-3148	396.7	4
KRH-2731	9.2	0.9
KRH-3955	5.3	1

Next, the two cell lines were analyzed for SDF-1α-mediated chemotaxis activity; after 24 h of incubation, about 30% of both Jurkat and E6-1 migrated to the lower wells in the presence of the control medium. Since the value was the background for this chemotaxis assay, we subtracted this value from the subsequent experiments. We decided to use 400 ng/mL of SDF-1α for the chemotaxis assay as previously described by Liang *et al.*[21] It was found that SDF-1α induced a four-fold increase in the migration efficiency of E6-1 cells compared to the original Jurkat cells (Fig. 1b). Therefore, we decided to use E6-1 cells for the subsequent experiments.

Next, we attempted to optimize the experimental conditions for the SDF-1α-mediated chemotaxis assay. The chemotaxis index plateaued at approximately 60% after 3 h incubation of E6-1 cells with 400 ng/mL of SDF-1α (data not shown). We then examined the effect of increasing concentration of SDF-1α on the chemotaxis index and found that the level of chemotaxis was augmented in a dose-dependent manner and plateaued when more than 40 ng/mL of SDF-1α was used (Fig. 1c). Accordingly, the optimal condition for the chemotaxis assay in subsequent experiments was 100 ng/mL of SDF-1α for a 3h incubation period.

Next, we analyzed the cytotoxicity of CXCR4 antagonists to E6-1 cells. As indicated in Figure 2(a), the CXCR4 antagonists were not cytotoxic for E6-1 cells at a 10 μM concentration. To ascertain the possibility of these antagonists also exhibiting agonistic activities, we examined the chemotaxis activity of the antagonists. We observed that 100 ng/mL SDF-1α efficiently induced migration of E6-1; however, none of antagonists induced migration even at 10 μM (Fig. 2b). This indicated that the CXCR4 antagonists did not possess agonistic properties.

The effect of CXCR4 antagonists on the chemotaxis was investigated under the same conditions as described above. The prototype antagonist KRH-1636 inhibited the SDF-1α-mediated chemotaxis up to approximately 40% at a maximal concentration (10 μM). By contrast, KRH-3148 almost completely inhibited the chemotaxis at the maximal concentration; moreover, KRH-2731 and KRH-3955 showed the maximum inhibition rate even at 1 μM (Fig. 3). In order to quantitatively compare these efficacies, 50% effective concentration (EC_{50}) was calculated (Table 1). The results from this study clearly showed that KRH-2731 and KRH-3955 were effective at >1000-fold as compared with KRH-1636.

We further evaluated the effect of the compounds on HIV-1 infection. Anti-HIV-1 activities in nM of KRH-1636, KRH-3148, KRH-2731, and KRH-3955, which were shown as EC_{50}, were 42, 4, 0.9, and 1, respectively (Table 1). The efficacy of the antagonists was highly correlated with their inhibitory effects on HIV-1 infection by interrupting the association of the Env with CXCR4. Interestingly, inhibition of chemotaxis by KRH-1636 and KRH-3148 was relatively lower than that of HIV-1 infection compared with KRH-2731 and KRH-3955. The difference may be because action sites of KRH-2731 or KRH-3955 against CXCR4 are somewhat different from those of KRH-3148 (Sei Kumakura, unpublished data). In summary, these results demonstrate that both KRH-2731 and KRH-3955 are capable of efficiently inhibiting SDF-1α-mediated chemotaxis as well as infection of T cell–tropic HIV-1.

Discussion

The present study demonstrated that the novel CXCR4 antagonists efficiently inhibited SDF-1α-mediated chemotaxis as well as

doi: 10.1111/j.1349-7006.2009.01104.x

infection of T cell-tropic HIV-1. Two compounds KRH-2731 and KRH-3955 were found to be highly potent inhibitors for both efficacies without any cytotoxicity or agonistic activity, indicating that they may be promising as anti-cancer metastasis and anti-HIV-1 drugs. In particular, both KRH-2731 and KRH-3955 efficiently inhibited calcium signaling induced by SDF-1α at a concentration of 10 nM, while KRH-3148 and KRH-1636 inhibited at 100 nM and at greater than 10 μM, respectively (Sei Kumakura *et al.*, unpublished results). This indicated that their antagonistic effects were highly correlated with their abilities to inhibit chemotaxis and HIV-1 infection.

While the Jurkat cell line expressed a smaller but almost comparable level of CXCR4 compared with E6-1 cells (Fig. 1a), their migration levels in the presence of SDF-1α were quite different (Fig. 1b). It is possible that the original Jurkat cells express non-functional CXCR4 with regard to signal transduction that is required for chemotaxis.

Tumor cells from various types of human cancers of epithelial, mesenchymal, and hematopoietic origins express high levels of CXCR4.[14,16] The interaction of SDF-1α with its receptor CXCR4 contributes to metastasis of breast cancer as well as a number of other malignancies in the lung, brain, and prostate. Furthermore, patients with cancers expressing high levels of CXCR4 have more extensive metastasis at lymph nodes compared with low CXCR4-expressing ones.[22] On this basis, the efficient CXCR4 antagonists demonstrated in this study may be highly valuable for the regulation of cancer metastasis. In fact, a synthetic peptide against CXCR4 efficiently inhibited metastasis of breast cancer in a mouse model,[21] thus providing support to our notion. However, a hurdle remains for the delivery of the peptide inihibitor to the primary focus of cancer in patients, thus impeding the clinical application of the inhibitor. In this regard, our low molecular weight CXCR4 antagonists are promising because they are non-cytotoxic and can be administered orally. In fact, KRH-3955 showed oral bioavailability of 25.6% in rats and its oral administration blocked X4 HIV-1 replication in the human peripheral blood lymphocytes and in severe combined immunodeficiency mouse system (Tsutomu Murakami *et al.*, manuscript in preparation). It is notable that AMD3100, another small non-peptide CXCR4 antagonist, has been shown to inhibit metastasis of cancer cells *in vitro* and *in vivo*.[23,24] Moreover, our preliminary data suggested that injection of the breast cancer cell line MDA-231 produced a huge tumor at the inoculated site as well as aggressive metastasis in the lungs of mice, and that our compounds partially inhibited both the primary tumor growth and the metastasis (data not shown).

In conclusion, CXCR4 antagonists, which can be orally administered, are promising agents for SDF-1α-mediated metastasis of cancer cells and also for the treatment and prophylaxis of a number of diseases related to the interaction between CXCR4 and SDF-1α, the best example of which would be an anti-HIV-1 drug.

Acknowledgments

We thank M. Kannagi and S. Yamaoka, Tokyo Medical and Dental University, for critical discussions. This work was supported by grants from the Ministry of Education, Culture, Sports, Science and Technology; the Ministry of Health, Labor and Welfare; and Human Health Science of Japan.

References

1 Ward SG, Westwick J. Chemokines: understanding their role in T-lymphocyte biology. *Biochem J* 1998; **333**: 457–70.
2 Le Y, Zhou Y, Iribarren P *et al.* Chemokines and chemokine receptors: their manifold roles in homeostasis and disease. *Cell Mol Immunol* 2004; **1**: 95–104.
3 Burger JA, Kipps TJ. CXCR4: a key receptor in the cross-talk between tumor cells and their microenvironment. *Blood* 2006; **107**: 1761–7.
4 Horuk R. Chemokine receptors. *Cytokine Growth Factor Rev* 2001; **12**: 313–15.
5 Nagasawa T, Hirota S, Tachibana K *et al.* Defects of B-cell lymphopoiesis and bone-marrow myelopoiesis in mice lacking the CXC chemokine PBSF/SDF-1. *Nature* 1996; **382**: 635–8.
6 Tachibana K, Hirota S, Iizasa H *et al.* The chemokine receptor CXCR4 is essential for vascularization of the gastrointestinal tract. *Nature* 1998; **393**: 591–4.
7 Zou YR, Kottmann AH, Kuroda M *et al.* Function of the chemokine receptor CXCR4 in haematopoiesis and in cerebellar development. *Nature* 1998; **393**: 595–9.
8 Burns JM, Summers BC, Wang Y *et al.* A novel chemokine receptor for SDF-1 and I-TAC involved in cell survival, cell adhesion, and tumor development. *J Exp Med* 2006; **203**: 2201–13.
9 Berger EA, Murphy PM, Farber JM. Chemokine receptors as HIV-1 coreceptors: roles in viral entry, tropism, and disease. *Annu Rev Immunol* 1999; **17**: 657–700.
10 Su L, Kaneshima H, Bonyhadi M *et al.* HIV-1-induced thymocyte depletion is associated with indirect cytopathogenicity and infection of progenitor cells in vivo. *Immunity* 1995; **2**: 25–36.
11 Bleul CC, Farzan M, Choe H *et al.* The lymphocyte chemoattractant SDF-1 is a ligand for LESTR/fusin and blocks HIV-1 entry. *Nature* 1996; **382**: 829–33.
12 Alkhatib G, Combadiere C, Broder CC *et al.* CC CKR5: a RANTES, MIP-1 alpha, MIP-1bata receptor as a fusion cofactor for macrophage-tropic HIV-1. *Science* 1996; **272**: 1955–8.
13 Cocchi F, DeVico AL, Garzino-Demo A *et al.* Identification of RANTES, MIP-1 alpha, and MIP-1 beta as the major HIV-suppressive factors produced by $CD8^+$ T cells. *Science* 1995; **270**: 1811–15.
14 Balkwill F. Cancer and the chemokine network. *Nature Rev Cancer* 2004; **4**: 540–50.
15 Luker KE, Luker GD. Functions of CXCL12 and CXCR4 in breast cancer. *Cancer Lett* 2006; **238**: 30–41.
16 Muller A, Homey B, Soto H *et al.* Involvement of chemokine receptors in breast cancer metastasis. *Nature* 2001; **410**: 50–6.
17 Liotta LA. An attractive force in metastasis. *Nature* 2001; **410**: 24–5.
18 Santiago B, Baleux F, Palao G *et al.* CXCL12 is displayed by rheumatoid endothelial cells through its base amino-terminal motif on heparan sulfate proteoglycans. *Arthritis Res Ther* 2006; **8**: R43.
19 Ichiyama K, Yokoyama-Kumakura S, Tanaka Y *et al.* A duodenally absorbable CXC chemokine receptor 4 antagonist, KRH-1636, exhibits a potent and selective anti-HIV-1 activity. *Proc Natl Acad Sci USA* 2003; **100**: 4185–90.
20 Tamamura H, Hori A, Kanzaki N *et al.* T140 analogs as CXCR4 antagonists identified as anti-metastatic agents in the treatment of breast cancer. *FEBS Lett* 2003; **550**: 79–83.
21 Liang Z, Wu T, Lou H *et al.* Inhibition of breast cancer metastasis by selective synthetic polypeptide against CXCR4. *Cancer Res* 2004; **64**: 4302–8.
22 Dewan MZ, Ahmed S, Iwasaki Y *et al.* Stromal cell-derived factor-1 and CXCR4 receptor interaction in tumor growth and metastasis of breast cancer. *Biomed Pharmacother* 2006; **60**: 273–6.
23 Yoon Y, Liang Z, Zhang X *et al.* CXC chemokine receptor-4 antagonist blocks both growth of primary tumor and metastasis of head and neck cancer in xenograft mouse models. *Cancer Res* 2007; **67**: 7518–24.
24 Li JK, Yu L, Shen Y *et al.* Inhibition of CXCR4 activity with AMD3100 decreases invasion of human colorectal cancer cells *in vitro*. *World J Gastroenterol* 2008; **14**: 2308–13.

総　　説

HIV 複製を制御する宿主因子の探索

Screenings for Host Factors That Regulate HIV Replication

村　上　　努
Tsutomu MURAKAMI
国立感染症研究所・エイズ研究センター
AIDS Research Center, National Institute of Infectious Diseases

キーワード：HIV，宿主因子，ゲノムワイド siRNA（shRNA）スクリーニング

はじめに

1996年より導入されたHAART療法はエイズによる死亡者数の顕著な減少に貢献してきた。しかしながら，薬剤耐性ウイルスの出現，重篤な副作用などの問題から，新規の作用点を持った薬剤の登場が望まれている。そのための有力なアプローチの一つがHIV-1とそれが利用する宿主因子の相互作用を阻害する薬剤の探索と開発である。このような理由に加えて，純粋にウイルス学的興味からもHIV-1の複製に関与する宿主因子に関する研究が種々の方法論によって行われてきた。中でも注目されたのは2008年から今年にかけては発表されたsiRNA（またはshRNA）による宿主因子のノックダウンに基づいたヒトの宿主因子に対する機能的ゲノムワイドスクリーニングによるHIV-1複製に必要な宿主因子の網羅的探索・同定の試みである。本稿ではHIV-1複製を制御する宿主因子の探索について，この機能的ゲノムワイドsiRNA（shRNA）スクリーニングを中心に概説する。

機能的ゲノムワイドsiRNA（shRNA）スクリーニング

昨年（2008年）ゲノムワイドにヒトの宿主因子をsiRNAトランスフェクションによってノックダウンし，HIV-1複製に対する影響をモニターすることによってHIV-1複製に必要な宿主因子を探索・同定する試みに関する報告が3つ報告された。最初の報告は2月のScience誌に発表された[1]。彼らはCD4を発現させ，Tatに反応するβ-galacotosidaseレポーター遺伝子を組み込んだHeLa細胞（TZM-bl細胞）にsiRNAのプール（1遺伝子当たり4個）をトランスフェクトし，72時間後に複製可能な感染性HIV-1（IIIB）を感染させた。まず，ウイルス感染の48時間後に細胞をp24カプシドに対して免疫染色し，HIV-1複製過程の主に前期過程に対する影響を評価した。さらに，ウイルス感染48時間後の培養上清を集め，あらたにTZM-bl細胞に感染させ24時間後にβ-galacotosidase活性を測定することによってsiRNA処理が感染性HIV-1粒子産生に与える影響も評価した。その結果，使用した21,121遺伝子のうち273遺伝子がコントロールと比較して2–3倍HIV-1の複製を阻害することが明らかになった。興味深いことに，このうち約1割の28遺伝子がウイルス複製の後期過程に作用すると推定された。また，今回見出されたHIV-1複製に関与する遺伝子の中で3つに絞って簡単な機能解析も同時に行われた。まず，小胞輸送に関与するRab蛋白質の一つRab6（ゴルジ装置の逆行輸送に関与することが知らせられている）がHIV-1と標的細胞への侵入過程に関与していることを示唆するデータを提示した（同時にやはりゴルジ装置の逆行輸送に関与するVps53についても同様の結果を得た）。次に，宿主因子の核移行に関与することが知られているTransportin 3-SR2（TNPO3）がHIV-1の核移行にも寄与していること，さらに，転写因子の一つであるMed28がそのノックダウンによってHIV-1の遺伝子発現は抑制するが，マウス白血病ウイルスの遺伝子発現には影響を与えないことを明らかにした。以上の3つの遺伝子のHIV-1複製過程への関与は新規な発見である。

昨年10月にはKönigらによって2番目の報告がCell誌に発表された[2]。彼らの研究成果は，主に以下の2つの点で前記の論文と異なっていた。すなわち，1）標的細胞が293T細胞であること，2）VSV-Gでシュードタイプしたluciferaseをレポーター遺伝子として組み込んだ複製欠損ウイルスを使用していることである。その結果，siRNAによる宿主因子のノックダウンによって評価されるのがHIV-1 Envによって行われる侵入過程を除く複製前期過程（脱殻，逆転写，ゲノムへの組込み）と転写・翻訳過程に限定されているのが特徴である。1遺伝子当たり6個のsiRNAを2個ずつまとめて（3ウェル/1遺伝子）をトランスフェク

著者連絡先：〒162-8640　東京都新宿区戸山1-23-1
2009年9月11日受付

トし，48時間後にVSV-Gでシュードタイプした複製欠損ウイルスを感染させた。まず，ウイルス感染の24時間後にレポーター遺伝子であるluciferaseの活性を測定してHIV-1複製過程の主に前期過程に対する影響を評価した。ウイルス複製阻害の特異性を評価するために，VSV-Gでシュードタイプしたマウス白血病ウイルス（MuLV）やアデノ随伴ウイルスについても同様の実験プロトコールで評価した。また，同時にsiRNAによるノックダウンによる細胞毒性も生細胞数測定により評価した。今回調べられた約20,000遺伝子のうち，複数のsiRNA処理によって細胞毒性を示すことなしにウイルスの感染価が45%以上減少した遺伝子は295個であった。興味深いことに，この295個の約80%はMuLVの複製にも影響を与えており，レトロウイルスで共通に利用できる宿主因子が多数あることが示唆された。295遺伝子のうち，44遺伝子が逆転写過程への関与が示され，そのうち12遺伝子は脱殻もしくは逆転写の開始に，23遺伝子はDNA合成のカイネティックスに影響を与えることが明らかになった。さらに，ウイルスDNAの核移行とインテグレーションに関与する遺伝子はそれぞれ6，9個示された。

Zouらによる3番目のsiRNAスクリーニングは，初めに述べたBrassらの方法によく似た方法を用いて行われた[3]。すなわち，CD4とCCR5を発現させ，β-galacotosidaseレポーター遺伝子を組み込んだHeLa細胞を標的細胞とし，siRNAのプール（1遺伝子当たり3個）をトランスフェクトし，24時間後に複製可能なHIV-1 HXB2株を感染させた。感染後48時間と96時間後のβ-galacotosidase活性を測定して，siRNAによるノックダウンの効果を評価した。感染後48時間のアッセイではウイルス複製前期過程（侵入，脱殻，逆転写，ゲノムへの組込み）と転写・翻訳過程についての評価を，感染後96時間ではウイルス粒子形成過程と未感染細胞への感染の拡がりをも含む複製過程全体に対する影響を検討した。スクリーニングの陽性コントロールにはCyclin T1（転写に関与；感染後48，96時間の両方でウイルス複製を阻害）とTSG101（出芽・放出に関与；感染後96時間でのみウイルス複製を阻害）に対するsiRNAを使用し，実験条件の最適化を行った。スクリーニングを行った19,709遺伝子のうち，確認実験やT細胞やマクロファージでの発現を考慮に入れて232遺伝子が候補遺伝子として選択された。その内訳は，ウイルス侵入に必要なCD4とCXCR4，Tatを介した転写活性化に関与する因子，ミトコンドリアの機能やエネルギー代謝に関係した因子などである。著者らはsiRNA非感受性のcDNA発現によるレスキュー実験なども行い，BAMP2キナーゼやDNA修復の関与するNEIL3がHIV-1の逆転写からゲノムへの組込みの過程に必要な因子であることも明らかにした。

2009年5月には，以上の3つのゲノムワイドなsiRNAスクリーニングを含む9つのHIV感染に重要な宿主因子のスクリーニングを対象としたメタ解析が報告された[4]。驚くべきことに，上記3つのスクリーニングの任意の2つのスクリーニング間でオーバーラップしていた遺伝子は最大でも7%以下であった。考えられる原因としては，実験条件（使用細胞やウイルス，siRNA処理の時間，感染を判定するタイミング）や候補遺伝子選定のフィルターの条件設定の違い，オフターゲット効果などが挙げられる。しかしながら，選択された遺伝子をその機能によってグループ分けしてみると（これをGene Ontology解析という），3つのスクリーニングで選択された遺伝子は，以下のような共通のグループに属していることが判明した。すなわち，核膜孔・核外（内）輸送，DNA修復，GTP結合，RNA結合，ユビキチン関連，mediator複合体，ER/Golgi輸送，プロテアソーム複合体，などである。

さらに最近，上記3つのスクリーニングの欠点であるHeLa（293T）細胞といった本来のHIV-1の標的細胞ではない材料を使用していた点を解消するためT細胞株（Jurkat細胞）を使用したshRNAを使用したゲノムワイドなスクリーニングの結果がYeungらによって報告された[5]。HIV-1の本来の標的細胞である初代CD4陽性T細胞に生理的条件が近いと考えられるJurkat細胞[6]にshRNAライブラリーを組み込んだレンチウイルスベクターを導入した。shRNAの発現した細胞を選択したのち，複製可能な感染性HIV-1クローン（NL4-3）を感染させた。Jurkat細胞はHIV-1の感染によって死滅するので，導入したshRNAがHIV-1感染に必要な宿主因子を十分にノックダウンした場合のみ細胞は生き残ることができる。この方法の特長は，上述したJurkat細胞を使用したことのほか，shRNAの発現した細胞を選択することによって，shRNAによるノックダウンが細胞毒性を示す遺伝子を排除できること，siRNAによる一時的なトランスフェクションに比べて長期間目的の遺伝子をノックダウンでき半減期の長い蛋白質に対してもウイルス複製への影響を明確に調べることが可能なことなどが挙げられる。54,509個のヒト転写産物をスクリーニングした結果，まずshRNA発現による長期的なノックダウンによって細胞毒性を示さなかったクローンが全体の約20%（9,357）得られ，このうちHIV-1の複製・産生を顕著に抑制した遺伝子252個が同定された。この252個はgene ontology解析の結果，いくつかの機能的なクラス（酵素結合，GTP結合，RNA結合など）に分類された。著者らは，この252個からランダムに22個を選び出し，1つの標的に対して5つのshRNAを作製しJurkat細胞に導入後，HIV-1複製の抑制活性を調べたところ，約半分のshRNA導入クローンで50-90%のウイルス複製抑制が観察された。さら